Institute for Advanced Simulation

Electronic Structure: Hartree-Fock and Correlation Methods

Christof Hättig

published in

Multiscale Simulation Methods in Molecular Sciences,
J. Grotendorst, N. Attig, S. Blügel, D. Marx (Eds.),
Institute for Advanced Simulation, Forschungszentrum Jülich,
NIC Series, Vol. **42**, ISBN 978-3-9810843-8-2, pp. 77-120, 2009.

http://www.fz-juelich.de/nic-series/volume42

Electronic Structure: Hartree-Fock and Correlation Methods

Christof Hättig

Lehrstuhl für Theoretische Chemie
Fakultät für Chemie und Biochemie
Ruhr-Universität Bochum, 44780 Bochum, Germany
E-mail: christof.haettig@rub.de

Hartree-Fock theory is the conceptually most basic electronic structure method and also the starting point for almost all wavefunction based correlation methods. Technically, the Hartree-Fock self-consistent field method is often also the starting point for the development of molecular Kohn-Sham density functional theory codes. We will briefly review the main concepts of Hartree-Fock theory and modern implementations of the Rothaan-Hall self-consistent field equations with emphasis on the techniques used to make these approaches applicable to large systems. The second part of the chapter will focus on wavefunction based correlation methods for large molecules, in particular second order Møller-Plesset perturbation theory (MP2) and, for calculations on excited states, the approximate coupled-cluster singles-and-doubles method CC2, both treating the electron-electron interaction correct through second order. It is shown how the computational costs (CPU time and storage requirements) can be reduced for these methods by orders of magnitudes using the resolution-of-the-identity approximation for electron repulsion integrals. The demands for the auxiliary basis sets are discussed and it shown how these approaches can parallelized for distributed memory architectures. Finally a few prototypical applications are reviewed.

1 Introduction

Today, essentially all efficient electronic structure methods are based on the Born-Oppenheimer approximation and molecular orbital theory. The Hartree-Fock method combines these two concepts with the variation principle and the simplest possible wave function ansatz obeying the Pauli exclusion principle: a Slater determinant or, for open-shell systems in restricted Hartree-Fock theory, a configuration state function. In spite of the fact that Hartree-Fock is since decades a matured quantum-chemical method, its implementation for large scale application is still today an active field of research. The reason for this is not that there is a large interest in the results from the Hartree-Fock calculations themselves. The driving force behind these developments are today the technical similarity between Hartree-Fock (HF) theory and Kohn-Sham density functional theory (DFT), in particular if hybrid functionals are used, and the fact that Hartree-Fock calculations are the starting point for almost all wavefunction based correlation methods. The challenge for HF and DFT implementations is today an efficient prescreening of the numerical important contributions and the storage of sparse matrices in large scale parallel calculations.

During the last decade also many wavefunction based correlation methods have been proposed for applications on extended molecular systems. Most of them are based on the so-called local correlation approach[1–9], and/or on an extensive screening of small but often long ranging contributions to the correlation energy[4,10,11]. Some approaches introduce empirical parameters or rely on a balance between certain contributions which in practice might or might not be given[12–15]. For most of these approaches it is not yet clear to

which extend they can be developed in the near future into competitive methods for extended systems. In particular, if the reduction of the computational costs (compared to more traditional implementations of quantum chemical methods) relies on a screening in the atomic orbital (AO) basis set, calculations on extended systems are often only possible with rather small basis sets which cannot supply the accuracy expected from a correlated *ab initio* method.[a] Even though usually only explored for electronic ground states, most of these approaches could in principle also be generalized to excited states. But for larger molecules, calculations for excited states employ often so-called response methods and the parameterization of the excited state used in these methods hampers the application of the local correlation and related approaches.[16–18]

We will in the following not go into the details of these approaches, but restrict ourself to discussion of to the underlying electronic structure methods, which are usually single-reference coupled-cluster (CC) and, in particular, for larger systems Møller-Plesset perturbation theory through second order (MP2) or related methods for excited states. The implementation of the latter methods has during the last decade improved dramatically by combining them with the so-called resolution-of-the-identity (RI) approximation for the four-index electron repulsion integrals (ERIs) with optimized auxiliary basis sets. Even without any further approximations are these methods today applicable to systems with up to 100 or more atoms. Since the RI approximation depends little on the electronic structure of the investigated system it does not diminish the applicability of the underlying electronic structure methods. It is also compatible and can be combined with the above mentioned screening based approaches to reduce further the computational costs.[19,20] Thus, it can be expected that these two aspects, the treatment of the electron correlation through second order and the RI approximation for ERIs will remain important ingredients also in future correlated wavefunction based methods for extended systems.

In the following the theory of wavefunction based ab initio methods that treat the electron-electron interaction correctly through second order is briefly reviewed. The emphasis will be on methods for excited states which can be related to the approximate coupled-cluster singles-and-doubles model CC2, an approximation to the coupled-cluster singles-and-doubles method (CCSD). In Sec. 7 it is shown how the computational costs for these methods can be reduced drastically by using the RI approximation and disc space bottlenecks for these methods can be resolved by an doubles amplitudes-direct implementation. A recent parallel implementation for distributed memory architectures is presented in Sec. 8 and some example applications with RI-MP2 and RI-CC2 are reviewed in Secs. 9 and 10.

2 The Born-Oppenheimer Approximation and the Electronic Schrödinger Equation

An important simplification in the quantum mechanical description of molecules, which is ubiquitously applied in electronic structure calculations is the Born-Oppenheimer (BO) approximation which leads to a separation of the electronic from the nuclear degrees of

[a] Here and in the following we use "ab initio" for electronic structure methods which are systematically improvable in the sense that they are members of a hierarchy which converges to the exact solution of the electronic Schrödinger equations, i.e. the full configuration interaction (Full CI) limit.

freedom. In the BO approximation the total Hamiltonian of molecular system is split in the operator for the kinetic energy $\hat{T}_{nuc}$ of the nuclei and the remaining contributions which are put into an electronic Hamiltonian $\hat{H}_{el}$.

$$\hat{H}_{tot} = \hat{T}_{nuc} + \hat{H}_{el} \tag{1}$$

In the non-relativistic case we have

$$\hat{T}_{nuc} = -\sum_{A} \frac{1}{2M_A} \hat{\nabla}_A^2 \tag{2}$$

and the electronic Hamiltonian can be written in atomic units as

$$\hat{H}_{el}(\mathbf{r}, \mathbf{R}) = -\sum_{i} \frac{1}{2} \hat{\nabla}_i^2 - \sum_{i,A} \frac{Z_A}{|\mathbf{R}_A - \mathbf{r}_i|} + \sum_{i<j} \frac{1}{|\mathbf{r}_i - \mathbf{r}_j|} + \sum_{A<B} \frac{Z_A Z_B}{|\mathbf{R}_A - \mathbf{R}_B|} \,, \tag{3}$$

where $\hat{\nabla}_A$ and $\hat{\nabla}_i$ are the gradients with respect to the coordinates of nucleus A and electron i, respectively, $\mathbf{R}_A$ and $\mathbf{r}_i$, and Z_A the charge of nucleus A.

The total wavefunction is approximated as product of an electronic and a nuclear wavefunction

$$\Psi_{tot}(\mathbf{r}, \mathbf{R}) \approx \Psi_{el}(\mathbf{r}, \mathbf{R}) \Psi_{nuc}(\mathbf{R}) \,. \tag{4}$$

where the electronic wavefunction is determined as eigenfunction of the electronic Hamiltonian

$$\hat{H}_{el}(\mathbf{r}, \mathbf{R}) \Psi_{el}(\mathbf{r}, \mathbf{R}) = E_{el}(\mathbf{R}) \Psi_{el}(\mathbf{r}, \mathbf{R}) \,, \tag{5}$$

and the nuclear wavefunction as solution of a nuclear Schrödinger equation

$$\Big(\hat{T}_{nuc} + E_{el}(\mathbf{R})\Big) \Psi_{nuc}(\mathbf{r}, \mathbf{R}) = E_{tot} \Psi_{nuc}(\mathbf{r}, \mathbf{R}) \,, \tag{6}$$

in which the eigenvalues of the electronic Hamiltonian, $E_{el}(\mathbf{R})$, appear as potential for the nuclear motion. It is therefore that we speak of $E_{el}(\mathbf{R})$ as potential energy surfaces. Our understanding of molecular structures as equilibrium positions on potential energy surfaces are implicit results of the Born-Oppenheimer approximation.

One may ask, what are the errors of the BO approximation? Beside the simplified wavefunction ansatz, Eq. (4), one neglects the so-called non-adiabatic coupling elements[b]:

$$\mathbf{A}^{(A)}(\vec{R}) = \int \Psi_{el}(\mathbf{r}, \mathbf{R})^* \Big(\hat{\nabla}_A \Psi_{el}(\mathbf{r}, \mathbf{R})\Big) d\mathbf{r} \tag{7}$$

$$B^{(A)}(\vec{R}) = \int \Psi_{el}(\mathbf{r}, \mathbf{R})^* \Big(\hat{\nabla}_A^2 \Psi_{el}(\mathbf{r}, \mathbf{R})\Big) d\mathbf{r} \tag{8}$$

There appear if the total Hamiltonian is applied to Ψ_{tot},

$$\begin{aligned} \hat{H}_{tot}\Psi_{tot} &= \hat{H}_{el}\Psi_{el}(\mathbf{r}, \mathbf{R})\Psi_{nuc}(\mathbf{R}) + \Psi_{el}(\mathbf{r}, \mathbf{R})\hat{T}_{nuc}\Psi_{nuc}(\mathbf{R}) \\ &\quad - \sum_{A} \frac{1}{2M_A} \Big\{ 2\Big(\hat{\nabla}_A \Psi_{el}(\mathbf{r}, \mathbf{R}\Big) \cdot \Big(\hat{\nabla}_A \Psi_{nuc}(\mathbf{R})\Big) + \Big(\hat{\nabla}_A^2 \Psi_{el}(\mathbf{r}, \mathbf{R}\Big) \Psi_{nuc}(\mathbf{R}) \Big\} \\ &= E_{tot}\Psi_{tot} \,, \end{aligned} \tag{9}$$

[b] Note that $\mathbf{A}^{(A)}(\vec{R})$ is a three-dimensional vector in the coordinate space of nucleus A, while $B^{(A)}(\vec{R})$ is scalar.

after integration over the electronic degrees of freedom:

$$\hat{H}_{tot}\Psi_{nuc} = \left(\hat{T}_{nuc} + E_{el}(\vec{R})\right)\Psi_{nuc} \qquad (10)$$
$$- \sum_A \frac{1}{2M_A}\left\{2\mathbf{A}^{(A)}(\mathbf{R})\cdot\hat{\nabla}_A + B^{(A)}(\mathbf{R})\right\}\Psi_{nuc} = E_{tot}\Psi_{nuc}$$

The nuclear Schrödinger equation in Eq. (6) is obtained by neglecting in the last equation the non-adiabatic coupling elements $\mathbf{A}^{(A)}(\mathbf{R})$ and $B^{(A)}(\mathbf{R})$. The errors introduced by the Born-Oppenheimer approximation are typically in the order of 0.1 kJ/mol and for the majority of applications today completely negligible compared to other errors made in the solution of the electronic and nuclear Schrödinger equations, Eqs. (5) and (6).

3 Slater Determinants

The Pauli principle requires that the electronic wavefunction Ψ_{el} is antisymmetric under any permutation of two electrons i and j,

$$\hat{P}_{ij}\Psi_{el}(\mathbf{r}_1,\ldots,\mathbf{r}_i,\ldots,\mathbf{r}_j,\ldots) = \Psi_{el}(\mathbf{r}_1,\ldots,\mathbf{r}_j,\ldots,\mathbf{r}_i,\ldots) \qquad (11)$$
$$= -\Psi_{el}(\mathbf{r}_1,\ldots,\mathbf{r}_i,\ldots,\mathbf{r}_j,\ldots)\,.$$

The simplest ansatz fulfilling this condition are Slater determinants, antisymmetrized products of one-electron wavefunctions (orbitals):

$$\Psi_{SD} = \tfrac{1}{\sqrt{n}}\hat{\mathcal{A}}\psi_1(\mathbf{r}_1)\ldots\psi_n(\mathbf{r}_n) = \begin{vmatrix} \psi_1(\mathbf{r}_1) & \psi_1(\mathbf{r}_2) & \ldots & \psi_1(\mathbf{r}_n) \\ \psi_2(\mathbf{r}_1) & \psi_2(\mathbf{r}_2) & \ldots & \psi_2(\mathbf{r}_n) \\ \vdots & \vdots & \ddots & \vdots \\ \psi_n(\mathbf{r}_1) & \psi_n(\mathbf{r}_2) & \ldots & \psi_n(\mathbf{r}_n) \end{vmatrix} \qquad (12)$$

The non-symmetrized orbital products are also known as Hartree products and will in the following be denoted by Θ.

$$\Psi_{SD} = \tfrac{1}{\sqrt{n}}\hat{\mathcal{A}}\Theta \qquad \text{with} \quad \Theta(\mathbf{r}_1,\ldots,\mathbf{r}_n) = \psi_1(\mathbf{r}_1)\ldots\psi_n(\mathbf{r}_n) \qquad (13)$$

The antisymmetrizer $\hat{\mathcal{A}}$ is defined as

$$\hat{\mathcal{A}} = \sum_{m=1}^{n!} \mathrm{sign}(P_m)\hat{P}_m \qquad (14)$$

where $\hat{P}_m$ is an operator which performs one of the $n!$ possible permutations of the n electrons and $\mathrm{sign}(P_m)$ the parity of this permutation. The group permutation operators has the property that if the whole set of all $n!$ possible permutations of n elements $\{\hat{P}_1,\hat{P}_2,\ldots,\hat{P}_{n!}\}$ is multiplied with some permutation $\hat{P}_k$ the same set of operators is recovered, just in a different order[c]:

$$\{\hat{P}_k\hat{P}_1,\hat{P}_k\hat{P}_2,\ldots,\hat{P}_k\hat{P}_{n!}\} = \{\hat{P}_1,\hat{P}_2,\ldots,\hat{P}_{n!}\}\,. \qquad (15)$$

Furthermore, the permutation operators $\hat{P}_m$ are unitary

$$\hat{P}_m^\dagger = \hat{P}_m^{-1} \qquad (16)$$

[c]This relation is in group theory known as rearrangement theorem.

where $\hat{P}_m^{-1}$ is the operator which performs the inverse permutation which has the same parity as P_m, i.e. $\mathrm{sign}(P_m) = \mathrm{sign}(P_m^{-1})$ and

$$\{\hat{P}_1^{-1}, \hat{P}_2^{-1}, \ldots, \hat{P}_{n!}^{-1}\} = \{\hat{P}_1, \hat{P}_2, \ldots, \hat{P}_{n!}\} \,. \tag{17}$$

From these relations it follows that the antisymmetrizer $\hat{\mathcal{A}}$ is an hermitian operator

$$\hat{\mathcal{A}}^\dagger = \sum_m \mathrm{sign}(P_m)\hat{P}_m^\dagger = \sum_m \mathrm{sign}(P_m^{-1})\hat{P}_m^{-1} = \hat{\mathcal{A}} \,, \tag{18}$$

and

$$\hat{\mathcal{A}}^2 = n!\hat{\mathcal{A}} \,. \tag{19}$$

Both relations are useful for evaluating matrix elements (integrals) for slater determinants. In the following we skip for convenience the index el for the electronic Hamiltonian and write it as

$$\hat{H} = E_{nuc} + \sum_i \hat{h}_i + \sum_{i<j} \frac{1}{r_{ij}} \tag{20}$$

with the nuclear repulsion energy and the one-electron hamiltonian defined as

$$E_{nuc} = \sum_{A<B} \frac{Z_A Z_B}{|\mathbf{R}_A - \mathbf{R}_B|} \,, \tag{21}$$

and

$$\hat{h}_i = -\frac{1}{2}\hat{\nabla}_i^2 - \sum_A \frac{Z_A}{|\mathbf{R}_A - \mathbf{r}_i|} \,, \tag{22}$$

and the interelectronic distances $r_{ij} = |\mathbf{r}_i - \mathbf{r}_j|$. Note that, because the summations are over all electrons or electron pairs, the antisymmetrizer $\hat{\mathcal{A}}$ commutes separately with the one- and two-electron contributions to the Hamiltonian $\hat{H}$:

$$\sum_i \hat{h}_i \hat{\mathcal{A}} = \hat{\mathcal{A}} \sum_i \hat{h}_i \qquad \text{and} \qquad \sum_{i<j} \frac{1}{r_{ij}} \hat{\mathcal{A}} = \hat{\mathcal{A}} \sum_{i<j} \frac{1}{r_{ij}} \tag{23}$$

For operators of this form we can rewrite the matrix elements for Slater determinants as

$$\begin{aligned} \big\langle \Psi_{SD,I} \big| \hat{O} \big| \Psi_{SD,J} \big\rangle &= \big\langle \tfrac{1}{\sqrt{n!}} \hat{A}\Theta_I \big| \hat{O} \big| \tfrac{1}{\sqrt{n!}} \hat{A}\Theta_J \big\rangle = \tfrac{1}{n!} \big\langle \hat{A}\Theta_I \big| \hat{A}\hat{O} \big| \Theta_J \big\rangle \\ &= \tfrac{1}{n!} \big\langle \hat{A}^2\Theta_I \big| \hat{O} \big| \Theta_J \big\rangle = \big\langle \hat{A}\Theta_I \big| \hat{O} \big| \Theta_J \big\rangle \end{aligned} \tag{24}$$

The results have, however, only a simple form if the orbitals ψ_i are orthogonal to each other. We will therefore in the following without loss of generality assume that Θ_I and Θ_J are build from a common set of orthonormal orbitals

$$\langle \psi_i | \psi_j \rangle = \delta_{ij} \tag{25}$$

and that the orbitals are ordered in the Hartree products according to increasing indices:

$$\Theta_I = \psi_{I_1}(\mathbf{r}_1)\psi_{I_2}(\mathbf{r}_2)\ldots\psi_{I_n}(\mathbf{r}_n) \qquad \text{with } I_1 < I_2 < \ldots < I_n \tag{26}$$

Overlap integrals then become

$$\left\langle \hat{A}\Theta_I \middle| \Theta_J \right\rangle = \sum_{m=1}^{n!} \mathrm{sign}(P_m) \prod_{k=1}^{n} \langle \psi_{I_{P_m(k)}} | \psi_{J_k} \rangle = \sum_{m=1}^{n!} \mathrm{sign}(P_m) \prod_{k=1}^{n} \delta_{I_{P_m(k)}, J_k} \tag{27}$$

where $P_m(k)$ is the result at position k after applying the permutation P_m because of Eq. (26) only the identity permutation can contribute to the result which is nonzero only if in both Hartree products exactly the same orbitals are occupied. We thus find that

$$\left\langle \Psi_{SD,I} \middle| \Psi_{SD,J} \right\rangle = \left\langle \hat{A}\Theta_I \middle| \Theta_J \right\rangle = \delta_{I,J} \tag{28}$$

Similarly, one obtains for the matrix elements of one-electron operators:

$$\left\langle \hat{A}\Theta_I \middle| \sum_i \hat{h}_i \middle| \Theta_J \right\rangle = \sum_{m=1}^{n!} \mathrm{sign}(P_m) \sum_{i=1}^{n} \langle \psi_{I_{P_m(i)}} | \hat{h}_i | \psi_{J_i} \rangle \prod_{\substack{k=1 \\ k \neq i}}^{n} \langle \psi_{I_{P_m(k)}} | \psi_{J_k} \rangle \, . \tag{29}$$

For an orthonormal orbital basis the matrix elements between two Slater determinants thus become:

$$\left\langle \Psi_{SD,I} \middle| \sum_i \hat{h}_i \middle| \Psi_{SD,J} \right\rangle = \begin{cases} \sum_{k=1}^{n} \langle \psi_{I_k} | \hat{h}_k | \psi_{I_k} \rangle & \text{for } I = J \\ \langle \psi_k | \hat{h} | \psi_l \rangle & \text{if } \Psi_{SD,I}, \Psi_{SD,J} \text{ differ only in } \psi_k, \psi_l \\ 0 & \text{otherwise} \end{cases} \tag{30}$$

Nonvanishing matrix elements are obtained if the two Slater determinants are identical or differ at most in one orbital. The matrix elements for the two-electron operators become:

$$\begin{aligned} \left\langle \Psi_{SD,I} \middle| \sum_{i<j} \tfrac{1}{r_{ij}} \middle| \Psi_{SD,J} \right\rangle &= \left\langle \hat{A}\Theta_I \middle| \sum_{i<j} \tfrac{1}{r_{ij}} \middle| \Theta_J \right\rangle \\ &= \sum_{m=1}^{n!} \mathrm{sign}(P_m) \sum_{i<j}^{n} \langle \psi_{I_{P_m(i)}} \psi_{I_{P_m(j)}} | \tfrac{1}{r_{ij}} | \psi_{J_i} \psi_{J_j} \rangle \\ &\quad \times \prod_{\substack{k=1 \\ k \neq i,j}}^{n} \langle \psi_{I_{P_m(k)}} | \psi_{J_k} \rangle \, , \end{aligned} \tag{31}$$

which reduces for orthonormal orbitals to:

$$\left\langle \Psi_{SD,I} \middle| \sum_{i<j} \tfrac{1}{r_{ij}} \middle| \Psi_{SD,J} \right\rangle = \begin{cases} \sum_{k<l}^{n} \langle \psi_{I_k} \psi_{I_l} || \psi_{I_k} \psi_{I_l} \rangle & \text{for } I = J \\ \sum_{m} \langle \psi_k \psi_{I_m} || \psi_l \psi_{I_m} \rangle & \text{if } \Psi_{SD,I}, \Psi_{SD,J} \text{ differ only in } \psi_k, \psi_l \\ \langle \psi_i \psi_j || \psi_k \psi_l \rangle & \text{if } \Psi_{SD,I}, \Psi_{SD,J} \text{ differ in } \psi_i, \psi_k \text{ and } \psi_j, \psi_m \\ 0 & \text{otherwise} \end{cases} \tag{32}$$

For two-electron operators non-vanishing matrix elements are obtained for Slater determinants which differ in up to two orbitals. The antisymmetrized integrals introduced on right side of Eq. (32) are defined as:

$$\langle \psi_i \psi_j || \psi_k \psi_l \rangle = (\psi_i \psi_k | \psi_j \psi_l) - (\psi_i \psi_l | \psi_j \psi_k) \,, \tag{33}$$

with the two-electron integrals in the Mulliken notation given by

$$(\psi_i \psi_j | \psi_k \psi_l) = \int_{\mathbb{R}^3} \int_{\mathbb{R}^3} \psi_i^*(\mathbf{r}_1) \psi_j(\mathbf{r}_1) \frac{1}{r_{12}} \psi_k^*(\mathbf{r}_2) \psi_l^*(\mathbf{r}_2) \, d\mathbf{r}_1 \, d\mathbf{r}_2 \,. \tag{34}$$

The expectation value of the total electronic Hamiltonian for a Slater determinant with the orthonormal occupied orbitals $\psi_1, \ldots, \psi_n$ is thus given by:

$$\big\langle \Psi_{SD} \big| \hat{H} \big| \Psi_{SD} \big\rangle = E_{nuc} + \sum_i \big\langle \psi_i \big| \hat{h} \big| \psi_i \big\rangle + \frac{1}{2} \sum_{ij} \big\langle \psi_i \psi_j \big|\big| \psi_i \psi_j \big\rangle \,. \tag{35}$$

4 Hartree-Fock Theory and the Roothaan-Hall Equations

The basic idea behind Hartree-Fock theory is to take the simplest meaningful ansatz for the electronic wavefunction, a Slater determinant, and to determine the occupied orbitals by the variation principle, i.e. such that energy expectation value is minimized. For general molecular or extended systems this scheme is usually combined with a basis set expansion of the molecular orbitals.

$$\psi_i(1) = \sum_{\nu=1}^{N} \chi_\nu(\mathbf{r}_1) C_{\nu i} \cdot \begin{cases} \alpha(1) \\ \beta(1) \end{cases} \,, \tag{36}$$

where $\{\chi_\nu\}$ is a basis set with N spatial functions and α und β are spin function for, respectively, the "spin up" and "spin down" states. For extended systems often plane wave basis sets is used, but for molecular systems local atom centered basis sets (*linear combination of atomic orbitals*, LCAO) are more common.

To minimize the Hartree-Fock energy with respect to the MO coefficients $c_{\nu i}$ under the constraint that the ψ_i are orthonormal we introduce the Lagrange function,

$$L_{\mathrm{HF}} = E_{nuc} + \sum_i \big\langle i \big| \hat{h} \big| i \big\rangle + \frac{1}{2} \sum_{ij} \big\langle ij \big|\big| ij \big\rangle + \sum_{ij} \epsilon_{ji} \big(\delta_{ij} - \big\langle i \big| j \big\rangle \big) \,. \tag{37}$$

Here and in the following we skip for notational convenience the functions ψ and χ in the brackets and give only there indices with the convention that $i, j, \ldots$ denote occupied MOs and greek indices AOs. The Lagrange function L_{HF} is now required to be stationary with respect to arbitrary variations of the MO coefficients[d]:

$$\frac{dL_{\mathrm{HF}}}{dC_{\nu i}^*} = \big\langle \nu \big| \hat{h} \big| i \big\rangle + \sum_k \big\langle \nu k \big|\big| i k \big\rangle - \sum_j \epsilon_{ji} \big\langle \nu \big| j \big\rangle = 0 \,. \tag{38}$$

[d] Requiring the derivatives $dL_{\mathrm{HF}}/dC_{\nu i}$ to vanish leads to equivalent complex conjugated equations.

We now introduce the Fock and overlap matrices in atomic orbital basis $\{\chi_\nu\}$ as:

$$F_{\mu\nu} = \big\langle \mu \big| \hat{h} \big| \nu \big\rangle + \sum_k \big\langle \mu k \big|\big| \nu k \big\rangle \tag{39}$$

$$= \big\langle \mu \big| \hat{h} \big| \nu \big\rangle + \sum_{\kappa\lambda} D_{\kappa\lambda} \Big\{ \big(\mu\nu\big|\kappa\lambda\big) - \big(\mu\lambda\big|\kappa\nu\big) \Big\} , \tag{40}$$

and

$$S_{\mu\nu} = \big\langle \mu \big| \nu \big\rangle , \tag{41}$$

with AO density matrix $\mathbf{D}$ defined as:

$$D_{\kappa\lambda} = \sum_k C^*_{\kappa k} C_{\lambda k} . \tag{42}$$

Note that the Hartree-Fock energy can be calculated from the Fock and densities matrices and the matrix of elements of the one-electron hamiltonian $h_{\mu\nu} = \langle \mu | \hat{h} | \nu \rangle$ as

$$E_{\mathrm{HF}} = \frac{1}{2} \sum_{\mu\nu} D_{\mu\nu} \Big(F_{\mu\nu} + h_{\mu\nu} \Big) . \tag{43}$$

With these intermediates Eq. (38) can be rewritten in a compact matrix form:

$$\mathbf{FC} = \mathbf{SC}\boldsymbol{\epsilon} . \tag{44}$$

The last equation is known under the name "Roothaan-Hall equation". Its meaning becomes more clear if it is transformed to an orthonormal basis set

$$\tilde{\chi}_\mu = \sum_\nu \chi_\nu [\mathbf{S}^{-1/2}]_{\nu\mu} \qquad \text{with} \quad \mathbf{S}^{-1/2}\mathbf{S}^{-1/2} = \mathbf{S}^{-1} , \tag{45}$$

where $[\mathbf{S}^{-1/2}]_{\mu\nu}$ denotes[e] the element μ, ν of the matrix $\mathbf{S}^{-1/2}$. In this basis the Roothaan-Hall equations become

$$\sum_\nu \tilde{F}_{\mu\nu} \tilde{C}_{\nu i} = \sum_j \tilde{C}_{\mu j} \epsilon_{ji} \qquad \text{with} \quad \tilde{F} = \mathbf{S}^{-1/2}\mathbf{F}\mathbf{S}^{-1/2} \quad \text{and} \quad \tilde{C} = \mathbf{S}^{1/2}\mathbf{C} . \tag{46}$$

The result of the Fock matrix applied any occupied orbital is a linear combination of only occupied orbitals. This condition determines the occupied molecular orbitals only up to a unitary transformation of these orbitals among themselves, which leaves the Slater determinant, i.e. the Hartree-Fock wavefunction, unchanged.

The so-called canonical orbitals are obtained by choosing this unitary transformation such that the matrix with the lagrangian multipliers ϵ_{ji} becomes diagonal. Usually, the equation is then augmented by a similar condition for the complementary space of unoccupied or "virtual" orbitals. The Roothaan-Hall equations become then a generalized nonlinear eigenvalue problem—nonlinear since the Fock matrix $\mathbf{F}$ depends through the density matrix $\mathbf{D}$ on the solution of the equations. The standard algorithm to solve these equations is the self-consistent field procedure which can be sketched as follows:

1. Initially a start density matrix is guessed (or constructed from some start orbitals, e.g. from an extended Hückel calculation)

[e] Note that $[\mathbf{S}^{-1/2}]_{\mu\nu} \neq 1/\sqrt{S_{\mu\nu}}$.

2. The Fock matrix F and the total energy for the approximate density matrix are calculated using Eqs. (39) and (43).

3. The generalized eigenvalue problem Eq. (44) is solved to obtain a new set of MOs.

4. An improved density matrix is guessed from the present approximation for the MOs and the previous density matrices using some convergence acceleration procedure.

5. If the total energy, the MOs and the density are converged (i.e. self-consistent) the procedure is stopped, else one continuous with step 2.

The number of iterations needed to converge the self-consistent field procedure depends on the molecular system (in particular its HOMO-LUMO gap), the quality of the start guess and a lot on the method used to update the density matrix in step 4. A common choice is the direct inversion of iterative subspaced (DIIS) technique of Pulay[21,22].

5 Direct SCF, Integral Screening and Integral Approximations

Apart from the technique used to solve the Roothaan-Hall equations, i.e. to update the density matrix, a second technically demanding aspect is the construction of the Fock matrix. A naive implementation of Eq. (39) would require the calculation of $\approx \frac{1}{8}N^4$ two-electron integral, where N is the dimension of our basis set in Eq. (36). To achieve a useful accuracy, typically 10–30 basis functions are needed per atom. For many systems of interest in computational chemistry today with 100 and more atoms the number of two-electron integrals will even today exceed standard disc space capacities. Furthermore, a brute force summation over all integrals would be unnecessary costly in terms of CPU time: for local atom-center basis sets many of the two-electron integrals and, depending on the HOMO-LUMO gap, also of the density matrix are numerically negligible; in extended systems the number of numerically significant two-electron coulomb integrals will only grow with $\mathcal{O}(\mathcal{N}^2)$, where $\mathcal{N}$ is a measure of the system size. A solution to these problems is offered by the integral-direct SCF scheme in combination with integral prescreening:

- The two-electron integrals are not stored once on stored on file, but instead (re)calculated when needed and immediately contracted with the elements of the density matrix to increments of the Fock matrix. By exploiting the eightfold permutational symmetry

$$(\mu\nu|\kappa\lambda) = (\nu\mu|\kappa\lambda) = (\mu\nu|\lambda\kappa) = (\nu\mu|\lambda\kappa) = \tag{47}$$
$$(\kappa\lambda|\mu\nu) = (\kappa\lambda|\nu\mu) = (\lambda\kappa|\mu\nu) = (\lambda\kappa|\nu\mu) \tag{48}$$

  of the two-electron integrals, one can restrict the loop over the AO indices to $\mu < \nu$, and $\kappa < \lambda$ with $(\mu, \nu) < (\kappa, \lambda)$ and add for each two-electron integral the following

6 increments to the Fock matrix:

$$F_{\mu\nu} \leftarrow F_{\mu\nu} + 2D_{\kappa\lambda}(\mu\nu|\kappa\lambda) \tag{49}$$
$$F_{\kappa\lambda} \leftarrow F_{\kappa\lambda} + 2D_{\mu\nu}(\mu\nu|\kappa\lambda) \tag{50}$$
$$F_{\mu\lambda} \leftarrow F_{\mu\lambda} - D_{\nu\kappa}(\mu\nu|\kappa\lambda) \tag{51}$$
$$F_{\nu\lambda} \leftarrow F_{\nu\lambda} - D_{\mu\kappa}(\mu\nu|\kappa\lambda) \tag{52}$$
$$F_{\mu\kappa} \leftarrow F_{\mu\kappa} - D_{\nu\lambda}(\mu\nu|\kappa\lambda) \tag{53}$$
$$F_{\nu\kappa} \leftarrow F_{\nu\kappa} - D_{\mu\lambda}(\mu\nu|\kappa\lambda) \tag{54}$$

(Where we assumed for simplicity that all four AO indices are different, else the redundant increments have to be skipped.)

- To estimate whether a specific integral might be large enough to make a significant contribution to the Fock matrix one exploits e.g. the Schwarz condition[f]:

$$|(\mu\nu|\kappa\lambda)| \leq Q_{\mu\nu}Q_{\kappa\lambda} \qquad \text{with} \quad Q_{\mu\nu} = \sqrt{(\mu\nu|\mu\nu)}\,. \tag{55}$$

For a given index quadruple the integral $(\mu\nu|\kappa\lambda)$ needs only to be calculated if

$$Q_{\mu\nu}Q_{\kappa\lambda}D_{max} \geq \tau \tag{56}$$

where

$$D_{max} = \max\{2|D_{\mu\nu}|, 2|D_{\kappa\lambda}|, |D_{\nu\kappa}|, |D_{\mu\kappa}|, |D_{\nu\lambda}|, |D_{\mu\lambda}|\}\,, \tag{57}$$

and τ is a user-defined threshold that determines the numerical accuracy of the calculation. Only if the inequality is fulfilled any of the contributions to the Fock matrix in Eqs. (49) – (54) can become larger than the threshold τ. This technique is today standard in essentially all direct Hartree-Fock codes and also in molecular DFT codes for so-called Hybrid functional with an Hartree-Fock-like "exact exchange" contribution.

For large systems the integral-screening reduces the computational costs for the Fock matrix construction from $\mathcal{O}(\mathcal{N}^4)$ to $\mathcal{O}(\mathcal{N}^2)$. If we split the two-electron part of the Fock matrix into separate Coulomb and exchange contributions,

$$F_{\mu\nu} = h_{\mu\nu} + J_{\mu\nu} - K_{\mu\nu}\,, \tag{58}$$

with

$$J_{\mu\nu} = \sum_{\kappa\lambda} D_{\kappa\lambda}(\mu\nu|\kappa\lambda)\,, \qquad \text{and} \qquad K_{\mu\nu} = \sum_{\kappa\lambda} D_{\kappa\lambda}(\mu\lambda|\kappa\nu)\,, \tag{59}$$

the remaining $\mathcal{O}(\mathcal{N}^2)$ scaling is caused by the Coulomb contribution while for the exchange part the integral screening reduces the number of requires contributions asymptotically to $\mathcal{O}(\mathcal{N})$ if the HOMO-LUMO gap does not vanish and the density matrix becomes sparse. This becomes more clear if the parameter D_{max} for the Coulomb and exchange contributions to the Fock matrix are calculated separately:

$$\text{Coulomb:} \qquad D_{max,C} = \max\{2|D_{\mu\nu}|, 2|D_{\kappa\lambda}|\} \tag{60}$$
$$\text{exchange:} \qquad D_{max,X} = \max\{|D_{\nu\kappa}|, |D_{\mu\kappa}|, |D_{\nu\lambda}|, |D_{\mu\lambda}|\} \tag{61}$$

[f] The Schwarz condition for two-electron integrals is a special case of a Cauchy-Schwarz inequality for scalar products in vector space: $|\langle x, y\rangle| \leq ||x|| \cdot ||y||$ with $||x|| = \sqrt{\langle x, x\rangle}$.

The size of the absolute values of the density matrix elements $D_{\mu\nu}$ and of the quantities $Q_{\mu\nu}$ are correlated with the overlap of the basis functions χ_μ and χ_ν. Thus, $D_{max,C}$ becomes usually only small if also the integral $|(\mu\nu|\kappa\lambda)| \leq Q_{\mu\nu} \cdot Q_{\kappa\lambda}$ is small, while in the exchange case the density matrix elements contributing to $D_{max,X}$ have indices then the Q's and criterion $Q_{\mu\nu}Q_{\kappa\lambda}D_{max,X}$ will only be fulfilled if all four basis functions μ, ν, κ, and λ are close in space.

Also, for medium sized molecules or with basis sets which contain diffuse functions only modest computational savings obtained with this technique and the large costs for the individual two-electron integrals can hamper the applicability of Hartree-Fock self-consistent field calculations. An approximation which leads to a significant reduction of the computational costs for the Coulomb contribution to the Fock matrix construction is the resolution-of-the-identity approximation for the two-electron integrals which is also known as density fitting:

$$(\mu\nu|\kappa\lambda) \approx (\mu\nu|Q)\,[\mathbf{V}^{-1}]_{QP}\,(P|\kappa\lambda)\;, \tag{62}$$

where $(\mu\nu|Q)$ and V_{PQ} are, respectively, three- and two-center two-electron integrals:

$$(\mu\nu|Q) = \int_{\mathbb{R}^3}\int_{\mathbb{R}^3} \chi^*_\mu(\mathbf{r}_1)\chi_\nu(\mathbf{r}_2)\frac{1}{r_{12}}Q(\mathbf{r}_2)\,d\mathbf{r}_1 d\mathbf{r}_2\;, \tag{63}$$

$$V_{PQ} = (Q|P) = \int_{\mathbb{R}^3}\int_{\mathbb{R}^3} P(\mathbf{r}_1)\frac{1}{r_{12}}Q(\mathbf{r}_2)\,d\mathbf{r}_1 d\mathbf{r}_2\;. \tag{64}$$

Within this approximation the Coulomb matrix $J_{\mu\nu}$ can be calculated as:

$$\gamma_P = \sum_{\kappa\lambda}(P|\kappa\lambda)D_{\kappa\lambda} \tag{65}$$

$$\sum_Q V_{PQ}c_Q = \gamma_P \tag{66}$$

$$J_{\mu\nu} \approx \sum_Q (\mu\nu|Q)c_Q \tag{67}$$

Where Eq. (66) is linear equation system for c_Q. In combination with an integral screening based on the Schwarz inequality these three equations can also be implemented with an asymptotic scaling of $\mathcal{O}(\mathcal{N}^2)$, but a significant lower prefactor than the original method, since there are fewer two- and three-center two-electron integrals and the computational costs for them are lower than for the four-center two-electron integrals $(\mu\nu|\kappa\lambda)$. We optimized auxiliary basis sets $\{Q\}$, which are today available for several standard basis sets, the errors introduced by the RI approximation are insignificant compared to the basis incompleteness error of the LCAO expansion in Eq. (36).

6 Second Order Methods for Ground and Excited States

Second order Møller-Plesset perturbation theory is a conceptually simple and technically the most simplest ab initio correlation method. It can be derived by expanding the solution of the electronic Schrödinger equation as a Taylor series in the fluctuation potential (vide infra). This can be done either in the framework of configuration interaction theory or using the single-reference coupled-cluster ansatz for the wavefunction.[23] We will take here

the latter starting point to have a close connection to coupled-cluster response and related methods for excited states. In the coupled-cluster ansatz the wavefunction is parameterized as

$$|\mathrm{CC}\rangle = \exp(\hat{T})|\mathrm{HF}\rangle \tag{68}$$

with the cluster operator defined as

$$\hat{T} = \hat{T}_1 + \hat{T}_2 + \hat{T}_3 + \dots \tag{69}$$

where

$$\hat{T}_1 = \sum_{\mu_1} t_{\mu_1} \hat{\tau}_{\mu_1} = \sum_{ai} t_a^i \hat{\tau}_a^i \;, \quad \hat{T}_2 = \sum_{\mu_2} t_{\mu_2} \hat{\tau}_{\mu_2} = \sum_{aibj} t_{ab}^{ij} \hat{\tau}_{ab}^{ij} \;, \quad \dots \tag{70}$$

The coefficients t_{μ_i} are called cluster amplitudes and the excitation operators $\hat{\tau}_{\mu_i}$ generate all possible single, double, and higher excited determinants if applied on the ground state Hartree-Fock (HF) determinant $|\mathrm{HF}\rangle$. Here and in the following, we use the convention that indices i, j, ... denote occupied, a, b, ... virtual, and p, q, ... arbitrary molecular orbitals (MOs).

Inserting the ansatz (68) into the electronic Schrödinger equation and multiplying from the left with $\exp(-\hat{T})$ one gets

$$\exp(-\hat{T})\hat{H}\exp(\hat{T})|\mathrm{HF}\rangle = E|\mathrm{HF}\rangle \;. \tag{71}$$

Projecting the above form of the Schrödinger equation onto the HF determinant and a projection manifold of (suitable linear combinations of) excited determinants one obtains an expression for the ground state energy

$$E = \langle \mathrm{HF}|\exp(-\hat{T})\hat{H}\exp(\hat{T})|\mathrm{HF}\rangle = \langle \mathrm{HF}|\hat{H}\exp(\hat{T})|\mathrm{HF}\rangle \;, \tag{72}$$

and the cluster equations

$$0 = \langle \mu_i|\exp(-\hat{T})\hat{H}\exp(\hat{T})|\mathrm{HF}\rangle \;, \tag{73}$$

which determine the amplitudes t_{μ_i}. Since we have not yet made any approximation, the above equations still give the exact ground state solution of the electronic Schrödinger equation. Truncating the cluster operator (69) after the single ($\hat{T}_1$) and double ($\hat{T}_2$) excitations gives the coupled-cluster singles-and-doubles (CCSD) method, truncating it after $\hat{T}_3$ the CCSDT method, and so on.[g]

Expressions for Møller-Plesset perturbation theory are found by splitting the Hamiltonian into the Fock operator $\hat{F}$ as zeroth-order and the electron-electron fluctuation potential as first-order contribution to the Hamiltonian

$$\hat{H}^{(0)} = \hat{F} \;, \qquad \hat{H}^{(1)} = \hat{\Phi} = \hat{H} - \hat{F} \;, \tag{74}$$

and expanding Eqs. (72) and (73) in orders of the fluctuation potential. If the Brillouin-Theorem is fulfilled and $\langle_a^i|\hat{H}|\mathrm{HF}\rangle = 0$, i.e. for a closed-shell or an unrestricted open-shell Hartree-Fock (UHF) reference, the MP2 energy is obtained as

$$E_{\mathrm{MP2}} = \langle \mathrm{HF}|\hat{\Phi}\hat{T}_2^{(1)}|\mathrm{HF}\rangle = \sum_{aibj} t_{ab}^{ij} \langle \mathrm{HF}|\hat{\Phi}|_{ij}^{ab}\rangle \tag{75}$$

[g] Similar as in configuration interaction theory, a truncation after single excitations (CCS) does not give a useful method for the calculation of ground state energies. As follows from the Brillouin theorem $\langle_a^i|\hat{H}|\mathrm{HF}\rangle = 0$, the cluster equations have then for a closed-shell or an unrestricted open-shell reference determinant the trivial solution $t_a^i = 0$ and the CCS energy becomes equal the HF energy.

with

$$0 = \langle^{ab}_{ij}|[\hat{F}, \hat{T}_2^{(1)}] + \hat{\Phi}|\mathrm{HF}\rangle \quad \Leftrightarrow \quad t^{ij}_{ab} = \frac{\langle^{ab}_{ij}|\hat{\Phi}|\mathrm{HF}\rangle}{\epsilon_i - \epsilon_a + \epsilon_j - \epsilon_b} \tag{76}$$

where we assumed canonical molecular orbitals and ϵ_p are the orbital energies.

Møller-Plesset perturbation theory can not straightforwardly be applied to excited states, since wavefunctions for excited states usually require a multi-reference treatment. For reviews on multi-reference many-body perturbation theory and its application on electronically excited states see e.g. Refs. 24, 25. Correlated second order methods for the calculation of excitation energies based on a single-reference treatment for electronic ground states can, however, be derived within the framework of coupled-cluster response theory. The idea behind response theory is to study a system exposed to time-dependent external (e.g. electric) fields and to derive from the response of the wavefunction or density the frequency-dependent properties of the system—for example polarizabilities and hyperpolarizabilities. The latter properties have singularities whenever a frequency of a field becomes equal to the excitation energy of an allowed transition in the system. Thus, from the poles of frequency-dependent properties one can identify the excitation energies.

Consider a quantum mechanical system described in the unperturbed limit by the time-independent Hamiltonian[h] $\hat{H}^{(0)}$ which is perturbed by a time-dependent potential:

$$\hat{H}(t, \epsilon) = \hat{H}^{(0)} + \hat{V}(t, \epsilon) \, . \tag{77}$$

We assume that the perturbation $\hat{V}$ can be expanded as a sum over monochromatic Fourier components

$$\hat{V}(t, \epsilon) = \sum_j \hat{V}_j \epsilon_j e^{-i\omega_j t} \, , \tag{78}$$

where $\hat{V}_j$ are hermitian, time-independent one-electron operators (e.g. for an electric field the dipole operator), t the time and ϵ_j are the amplitudes of the associated field strengths. Then the full time-dependent wavefunction of the system, i.e. the solution to the time-dependent Schrödinger equation, can be expanded as a power series in the field strengths as

$$\Psi(t) = \underbrace{\left[\Psi^{(0)} + \sum_j \Psi_j^{(1)}(\omega_j)\epsilon_j e^{-i\omega_j t} + \dots\right]}_{\text{phase-isolated wavefunction } \tilde{\Psi}} e^{-i\int_{t_0}^{t} dt' \langle\tilde{\Psi}(t)|\hat{H}(t',\epsilon) - i\frac{\partial}{\partial t'}|\tilde{\Psi}(t)\rangle} \, , \tag{79}$$

and an expectation value for an operator $\hat{\mu}$ as

$$\langle\mu\rangle(t) = \langle\tilde{\Psi}(t)|\hat{\mu}|\tilde{\Psi}(t)\rangle = \mu^{(0)} + \sum_j \langle\langle\mu; V_j\rangle\rangle_{\omega_j} \epsilon_j e^{-i\omega_j t} + \dots \tag{80}$$

For detailed reviews of modern response theory and its implementation for approximate wavefunction methods the interested reader is referred to Refs. 26–31. The important point for the calculation excitation energies is that the poles in the response functions $\langle\langle\mu; V\rangle\rangle_\omega$ occur when ω becomes equal to an eigenvalue of the stability matrix of the employed

[h] Note that $\hat{H}^{(0)}$ includes here the fluctuation potential in difference to Eq. (74), where the fluctuation potential $\hat{\Phi}$ has been the perturbation.

electronic structure method for the unperturbed system. The stability matrix contains the derivatives of the residua of the equations which determine the wavefunction parameters with respect to these parameters. For Hartree-Fock, multi-configurational self-consistent field (MCSCF), density functional theory (DFT), configuration interaction (CI) or other methods which are variational in the sense that the wavefunction parameters are determined by minimization of the energy, the stability matrix is the so-called electronic Hesse matrix—the matrix of the second derivatives of the energy with respect to the wavefunction parameters. For coupled-cluster methods the cluster amplitudes are determined by the cluster equations (73). Arranging the residua in a vector function

$$\Omega_{\mu_i}(t_{\nu_i}) = \langle \mu_i | \exp(-\hat{T}) \hat{H} \exp(\hat{T}) | \mathrm{HF} \rangle \ , \tag{81}$$

the stability matrix is given by the Jacoby matrix

$$\mathbf{A}_{\mu_i \nu_j} = \left. \frac{d\Omega_{\mu_i}}{dt_{\nu_j}} \right|_{\epsilon=0} = \langle \mu_i | \exp(-\hat{T}) [\hat{H}, \hat{\tau}_{\nu_j}] \exp(\hat{T}) | \mathrm{HF} \rangle \ , \tag{82}$$

where $|_{\epsilon=0}$ indicates that the derivatives are taken for the unperturbed system, i.e. at zero field strengths. In configuration interaction theory the stability matrix becomes the matrix representation of the reduced Hamiltonian $\hat{H} - E_0$ (where E_0 is the ground state energy) in the space orthogonal to the electronic ground state.[i] In coupled-cluster theory this matrix representation is obtained in a similarity transformed basis.[j]

In this way excitation energies can in principle be derived for any electronic structure method. However, to obtain physical meaningful and accurate results, the method has to fulfill certain requirements. For example from the equations for the amplitudes in MP2, Eq. (76), one obtains a Jacoby matrix which gives only excitation energies corresponding to double excitations and these would be equal to the orbital energy differences in the denominator of the amplitudes. The two most important requirements are firstly, that there must be a one-to-one correspondence between the parameters of the wavefunction and at least the investigated part of the spectrum of the Hamiltonian. This requires methods which determine the time-dependent variables by a single set of equations, as e.g. time-dependent Hartree-Fock (HF-SCF), density functional theory (DFT) or multi-configuration self-consistent field (MCSCF, CASSCF, or RASSCF), but not a time-dependent configuration interaction (CI) treatment on top of a time-dependent HF-SCF calculation. For this reason the coefficients of the Hartree-Fock orbitals are also above in Eqs. (81) and (82) not considered as parameters of the time-dependent wavefunction, since this second set of variables in the time-dependent problem would lead to a second set of eigenvalues corresponding to single excited states, additionally to the one obtained from the parameterization through the singles cluster amplitudes. Instead, the time-dependent wavefunction is in coupled-cluster response theory usually constructed using the (time-independent) orbitals of the unperturbed system with time-dependent cluster amplitudes. Secondly, to obtain accurate results the stability matrix must also provide an accurate approximation of the those blocks of the Hamiltonian which are most important for the investigated states. For single excitations these are the singles-singles block $\mathbf{A}_{\mu_1 \nu_1}$ and the off-diagonal blocks

[i] In connection with CI and propagator methods (approximate) matrix representations of $\hat{H} - E_0$ are often also referred to as secular matrix.

[j] $\langle \mu_i | \exp(-\hat{T})$ for the bra and $\exp(\hat{T}) | \mu_j \rangle$ for the ket states, where $|\mu_j\rangle = \hat{\tau}_{\mu_j} |\mathrm{HF}\rangle$; for further details see e.g. Ref. 23

$\mathbf{A}_{\mu_2\nu_1}$ and $\mathbf{A}_{\mu_1\nu 2}$ next to it. With the usual single-reference coupled-cluster methods these blocks are described most accurately and therefore the excitation energies for single excitation dominated transitions are obtained with the highest accuracy, while excitation energies for double and higher excitations are usually considerably less accurate.

Already at the coupled-cluster singles (CCS) level (which for excitation energies is—in contrast to ground state calculations—not equivalent to Hartree-Fock, but to configuration interaction singles (CIS)), excitation energies for states dominated by single replacements of one spin-orbital in the Hartree-Fock reference determinant are obtained correctly through first order in the electron-electron interaction.

A second order method for excited states which accounts for the above requirements and takes over the accuracy of MP2 to excited states dominated by single excitations can be derived by approximating the cluster equations to lowest order in the fluctuation potential. But in difference to the derivation of MP2 in Eqs. (74) – (76) we allow in the Hamiltonian for an additional one-electron perturbation

$$\hat{H}(t) = \hat{F} + \hat{\Phi} + \hat{V}(t) \,, \tag{83}$$

which can induce transitions to single excitations and has, as necessary in CC response theory, not been included in the Hartree-Fock calculation. Because of the latter, single excitation amplitudes contribute now to the cluster operator already in zeroth order in the fluctuation potential, $\hat{\Phi}$, and in first order $\hat{T}_1$ and $\hat{T}_2$ both contribute to the wavefunction. Approximating the equations that determine these amplitudes to second (singles) and first order (doubles) one obtains the equations for the approximate coupled-cluster model CC2[32,33]:

$$0 = \langle_i^a|[\hat{\tilde{H}}, \hat{T}_2] + \hat{\tilde{H}}|\mathrm{HF}\rangle \,, \tag{84}$$

$$0 = \langle_{ij}^{ab}|[\hat{F}, \hat{T}_2] + \hat{\tilde{H}}|\mathrm{HF}\rangle \,, \tag{85}$$

where a similarity transformed Hamiltonian $\hat{\tilde{H}} = \exp(-\hat{T}_1)\hat{H}\exp(\hat{T}_1)$ has been introduced to obtain a compact notation. In difference to MP2 the equations for CC2 have to be solved iteratively because of the coupling introduced by $\hat{T}_1$. The ground state energy obtained from CC2

$$E_{\mathrm{CC2}} = \langle \mathrm{HF}|\hat{\Phi}(\hat{T}_2 + \tfrac{1}{2}\hat{T}_1\hat{T}_1)|\mathrm{HF}\rangle \,, \tag{86}$$

is, as for MP2, (only) correct through second order in the fluctuation potential[k], but it leads to a Jacoby matrix with the singles-singles block $\mathbf{A}_{\mu_1\nu_1}$ correct through second order and the off-diagonal blocks $\mathbf{A}_{\mu_1\nu_2}$ and $\mathbf{A}_{\mu_2\nu_1}$ correct through first-order in the fluctuation potential, while the doubles-doubles $\mathbf{A}_{\mu_2\nu_2}$ block is approximated by the zeroth-order term:

$$\mathbf{A}^{\mathrm{CC2}} = \begin{pmatrix} \langle_i^a|[(\hat{\tilde{H}} + [\hat{\tilde{H}}, \hat{T}_2]), \hat{\tau}_k^c|\mathrm{HF}\rangle & \langle_i^a|[\hat{\tilde{H}}, \hat{\tau}_{kl}^{cd}]|\mathrm{HF}\rangle \\ \langle_{ij}^{ab}|[\hat{\tilde{H}}, \hat{\tau}_k^c]|\mathrm{HF}\rangle & \langle_{ij}^{ab}|[\hat{F}, \hat{\tau}_{kl}^{cd}]|\mathrm{HF}\rangle \end{pmatrix} \,. \tag{87}$$

CC2 is the computational simplest iterative coupled-cluster model which gives single excitation energies which are correct through second order. Through the similarity transformed

[k] Therefore, CC2 does in general not describe ground state energies, structures, or properties more accurately than MP2. Its advantage upon MP2 is that, combined with coupled-cluster response theory, it can (in contrast to the latter) applied successfully to excited states.

Hamiltonian $\hat{\tilde{H}} = \exp(-\hat{T}_1)\hat{H}\exp(\hat{T}_1)$ the Jacoby matrix in Eq. (87) includes, however, also some higher-order terms, since for the unperturbed system the single excitation amplitudes t_{μ_1} contribute only in second- and higher orders to the ground state wavefunction.[l] Excluding these terms and replacing the doubles amplitudes by the first-order amplitudes, Eq. (76), from which the MP2 energy in calculated, one obtains the Jacoby matrix of the CIS(D_∞) approximation[37], an iterative variant of the perturbative doubles correction[38] CIS(D) to CIS (or CCS):

$$\mathbf{A}^{\mathrm{CIS(D_\infty)}} = \begin{pmatrix} \langle {}^a_i|[(\hat{H}+[\hat{H},\hat{T}_2]),\hat{\tau}^c_k|\mathrm{HF}\rangle & \langle {}^a_i|[\hat{H},\hat{\tau}^{cd}_{kl}]|\mathrm{HF}\rangle \\ \langle {}^{ab}_{ij}|[\hat{H},\hat{\tau}^c_k]|\mathrm{HF}\rangle & \langle {}^{ab}_{ij}|[\hat{F},\hat{\tau}^{cd}_{kl}]|\mathrm{HF}\rangle \end{pmatrix} . \tag{88}$$

This Jacobian contains the minimal number of terms required to obtain the excitation energies for single replacement dominated transitions correct through second order. However, it is not possible to construct a coupled-cluster model which leads exactly to such a Jacoby matrix.

The computational savings of CIS(D_∞) compared to CC2 are rather limited[37] and CC2 has, as a member of the hierarchy of coupled-cluster methods CCS, CC2, CCSD, CC3, CCSDT, ... certain conceptual advantages. The Jacoby matrix of the CIS($D\infty$) approximation may, however, used as starting point to derive the perturbative doubles correction CIS(D) to the CIS (or CCS) excitation energies[37]:

$$\omega^{(\mathrm{D})} = \sum_{\mu_1\nu_1} E^{\mathrm{CIS}}_{\mu_1} \left[\mathbf{A}^{\mathrm{CIS(D_\infty)}}_{\mu_1\nu_1} - \mathbf{A}^{\mathrm{CIS}}_{\mu_1\nu_1} + \sum_{\kappa_2} \frac{\mathbf{A}^{\mathrm{CIS(D_\infty)}}_{\mu_1\kappa_2}\mathbf{A}^{\mathrm{CIS(D_\infty)}}_{\kappa_2\nu_1}}{\omega^{\mathrm{CIS}} - \epsilon_{\kappa_2}} \right] E^{\mathrm{CIS}}_{\nu_1} \tag{89}$$

or

$$\omega^{\mathrm{CIS(D)}} = \omega^{\mathrm{CIS}} + \omega^{(\mathrm{D})} = \sum_{\mu_1\nu_1} E^{\mathrm{CIS}}_{\mu_1} \left[\mathbf{A}^{\mathrm{CIS(D_\infty)}}_{\mu_1\nu_1} + \sum_{\kappa_2} \frac{\mathbf{A}^{\mathrm{CIS(D_\infty)}}_{\mu_1\kappa_2}\mathbf{A}^{\mathrm{CIS(D_\infty)}}_{\kappa_2\nu_1}}{\omega^{\mathrm{CIS}} - \epsilon_{\kappa_2}} \right] E^{\mathrm{CIS}}_{\nu_1} \tag{90}$$

where ϵ_{κ_2} contains the orbital energy difference for a double excitation, $\epsilon^{ij}_{ab} = \epsilon_a - \epsilon_i + \epsilon_b - \epsilon_j$.

Another second order method for excited states which is related to CC2 and CIS(D) is the so-called algebraic diagrammatic construction through second order, ADC(2).[39,40] The secular matrix of ADC(2) is just the symmetric part of $\mathbf{A}^{\mathrm{CIS(D_\infty)}}$:

$$\mathbf{A}^{\mathrm{ADC(2)}} = \tfrac{1}{2}\mathbf{A}^{\mathrm{CIS(D_\infty)}} + \tfrac{1}{2}\left(\mathbf{A}^{\mathrm{CIS(D_\infty)}}\right)^\dagger , \tag{91}$$

which leads to some conceptual and also computational simplifications e.g. in the calculation of derivatives (gradients!) since the left and right eigenvectors of a symmetric matrix are identical, while for the non-symmetric Jacoby matrices of CC2 and CIS(D_∞) left and right eigenvectors differ. Both eigenvectors are needed for the calculation of derivatives. Other second order methods for excited states are the second order polarization propagator approach,[41,42] SOPPA and the perturbative doubles correction,[43] RPA(D), to time-dependent Hartree-Fock, which for excitation energies is also known as the random phase

[l] We assume here that the Brillouin theorem is fulfilled and thus the occupied/virtual block of the Fock matrix vanishes. This holds for closed-shell and unrestricted open-shell Hartree-Fock reference states. For a discussion of additional terms that need to be accounted for in restricted open-shell SCF based calculations we refer e.g. to Refs.[34–36].

approximation (RPA). The latter method can also be understood as a non-iterative approximation to SOPPA, similar as CIS(D) is a non-iterative approximation to CIS(D_∞). The relation of RPA(D) and SOPPA to the single-reference coupled-cluster response methods is somewhat more difficult, since these methods are members of a different hierarchy of methods (with RPA (TDHF) as first-order model) which is related to the so-called orbital-optimized coupled-cluster (OCC) methods[44,45]. Therefore, these methods will not be discussed in detail in the following, but we note that the same concepts (doubles amplitude-direct formulation and RI-approximation) can by applied to reduce also for these the computational costs to the same extend as for CC2, ADC(2), CIS(D_∞), and CIS(D).

6.1 Doubles amplitude-direct formulation of second order methods

An important feature of second order methods or approximate doubles methods, as one might also call them, is that an explicit storage (in RAM or on disk) of complete sets of double excitation amplitudes can be avoided similar as the storage of triples amplitudes is avoided in the approximate triples methods CCSD(T), CCSDT-1, CCSDR(3), or CC3.[46–49] This is important for applications on large molecules since similar as for the approximate triples methods the storage of the amplitudes would prohibit large-scale applications simply by a storage space or I/O bottleneck.

For example, the MP2 energy can be calculated without storing the double excitation amplitudes using the following scheme[m]:

```
do i = 1, nocc
  do j = i, nocc
    do a = 1, nvirt
      do b = b, nvirt
        t_ab^ij = (ia|jb)/(ε_i − ε_a + ε_j − ε_b)
        E_MP2 = E_MP2 + (2 − δ_ij){2(ia|jb) − (ia|jb)}t_ab^ij
      end do
    end do
  end do
end do
```

In a similar way also the equations for the doubles amplitudes in CC2 can—for given singles amplitudes t_a^i—immediately be inverted to

$$t_{ab}^{ij} = (ai\tilde{|}bj)/(\epsilon_i - \epsilon_a + \epsilon_j - \epsilon_b) \tag{92}$$

where the similarity transformation with $\exp(\hat{T}_1)$ has been included in the AO-to-MO transformation for the modified two-electron integrals

$$(ai\tilde{|}bj) = \sum_\alpha \Lambda_{\alpha a}^p \sum_\beta \Lambda_{\beta i}^h \sum_\gamma \Lambda_{\gamma b}^p \sum_\delta \Lambda_{\delta j}^h \, (\alpha\beta|\gamma\delta) \tag{93}$$

with $\Lambda_{\alpha a}^p = C_{\alpha a} - \sum_k C_{\alpha k} t_a^k$ and $\Lambda_{\alpha i}^h = C_{\alpha i} + \sum_c C_{\alpha c} t_c^i$. Inserting Eq. (92) into the equation for the singles amplitudes, Eq. (84), gives a set of effective equations for the CC2

[m] The explicit formulas given here and below are for a closed-shell restricted Hartree-Fock reference determinant.

singles amplitudes, which reference the doubles amplitudes t_{ab}^{ij} only as intermediates, which can be calculated and contracted with one- and two-electron integrals "on-the-fly" without storing a complete set of these amplitudes on disk:

```
do i = 1, nocc
  do j = 1, nocc
    do a = 1, nvirt
      do b = 1, nvirt
        t_ab^ij = (ai~|bj)/(ε_i - ε_a + ε_j - ε_b)
        Ω_ci = Ω_ci + Σ_abj (2t_ab^ij - t_ba^ij)(jb~|ca)
        Ω_ak = Ω_ak - Σ_bij (2t_ab^ij - t_ba^ij)(jb~|ik)
        ⋮
      end do
    end do
  end do
end do
```

To avoid the storage of doubles amplitudes is even more important for excited states, since in this case else doubles contributions to eigen- or trial vectors would have to be stored for several simultaneously solved eigenvalues and a number of iterations. An explicit reference to the doubles part of eigen- or trial vectors during the solution of the eigen problem can for the approximate doubles methods be removed by exploiting the particular structure of the Jacoby or secular matrices of these methods, in which the doubles-doubles block is in the canonical orbital basis diagonal with the diagonal elements equal to SCF orbital energy differences:

$$\begin{pmatrix} \mathbf{A}_{\mu_1\nu_1} & \mathbf{A}_{\mu_1\nu_2} \\ \mathbf{A}_{\mu_2\nu_1} & \delta_{\mu_2\nu_2}\epsilon_{\nu_2} \end{pmatrix} \begin{pmatrix} E_{\nu_1} \\ E_{\nu_2} \end{pmatrix} = \omega \begin{pmatrix} E_{\nu_1} \\ E_{\nu_2} \end{pmatrix} . \tag{94}$$

The doubles part of the eigenvectors is thus related to the singles part and the eigenvalue through the equation

$$E_{\mu_2} = \frac{\sum_{\nu_1} \mathbf{A}_{\mu_2\nu_1} E_{\nu_1}}{\omega - \epsilon_{\mu_2}} . \tag{95}$$

which allows to partition the linear eigenvalue problem in the space of singles and doubles replacements as an effective eigenvalue problem in the space of only the single excitations:

$$\sum_{\nu_1} \left[\mathbf{A}_{\mu_1\nu_1} + \sum_{\kappa_2} \frac{\mathbf{A}_{\mu_1\kappa_2}\mathbf{A}_{\kappa_2\nu_1}}{\omega - \epsilon_{\kappa_2}} \right] E_{\nu_1} = \sum_{\nu_1} \mathbf{A}^{eff}_{\mu_1\nu_1}(\omega) E_{\nu_1} = \omega E_{\mu_1} . \tag{96}$$

The last equation is, however, in difference to Eq. (94) a nonlinear eigenvalue problem because the effective Jacoby matrix $\mathbf{A}^{eff}_{\mu_1\nu_1}(\omega)$ depends on the eigenvalue ω, which is itself first known when the equation has been solved. But with iterative techniques this eigenvalue problem can be solved almost as efficiently as the original linear eigenvalue problem

and the elimination of the need to store the doubles part of solution or trial vectors more than compensates this complication.[50]

To apply these iterative techniques for the solution of large-scale eigenvalue problems one needs to implement matrix vector products of the form

$$\sigma_{\mu_1}(\omega, b_{\nu_1}) = \sum_{\nu_1} \mathbf{A}^{eff}_{\mu_1\nu_1}(\omega) b_{\nu_1} = \sum_{\nu_1} \mathbf{A}_{\mu_1\nu_1} b_{\nu_1} + \sum_{\kappa_2} \mathbf{A}_{\mu_1\kappa_2} \frac{\sum_{\nu_1} \mathbf{A}_{\kappa_2\nu_1} b_{\nu_1}}{\omega - \epsilon_{\kappa_2}} \,. \quad (97)$$

Note the similarity of the quotient in the last term with the expression in Eq. (95). For CC2 this term becomes

$$b^{ij}_{ab} = \frac{1}{\epsilon_{iajb}} \sum_{ck} \mathbf{A}_{iajb,kc} b^k_c = \frac{\sum_{ck} \langle {}^{ab}_{ij} | [\hat{\tilde{H}}, \hat{\tau}^k_c] | \mathrm{HF} \rangle b^k_c}{\epsilon_i - \epsilon_a + \epsilon_j - \epsilon_b + \omega} = \frac{2(ai|bj) - (bi|aj)}{\epsilon_i - \epsilon_a + \epsilon_j - \epsilon_b + \omega} \,, \quad (98)$$

with the modified MO electron repulsion integrals

$$(ai|\bar{bj}) = \hat{P}^{ij}_{ab} \sum_{\alpha\beta} \left(\bar{\Lambda}^p_{\alpha a} \Lambda^h_{\beta i} + \Lambda^p_{\alpha a} \bar{\Lambda}^h_{\beta i} \right) \sum_{\gamma\delta} \Lambda^p_{\gamma b} \Lambda^h_{\delta j} \, (\alpha\beta|\gamma\delta) \,, \quad (99)$$

where $\bar{\Lambda}^p_{\alpha a} = -\sum_k C_{\alpha k} b^k_a$, $\bar{\Lambda}^h_{\alpha i} = +\sum_c C_{\alpha c} b^i_c$ and $\hat{P}^{ij}_{ab}$ a symmetrization operator defined through $\hat{P}^{ij}_{ab} f_{ia,jb} = f_{ia,jb} + f_{jb,ia}$. The linear transformation in Eq. (97) can thus be calculated using a similar algorithm as for the residuum of the ground state cluster equations without storing any doubles vectors:

```
do i = 1, nocc
  do j = 1, nocc
    do a = 1, nvirt
      do b = 1, nvirt
        b^ij_ab = (ai|bj)/(ε_i − ε_a + ε_j − ε_b + ω)
        σ_ci = σ_ci + Σ_abj (2 b^ij_ab − b^ij_ba)(jb|ca)
        ⋮
        t^ij_ab = (ai|bj)/(ε_i − ε_a + ε_j − ε_b)
        σ_ai = σ_ai + Σ_bj (2 t^ij_ab − t^ij_ba) Σ_ck [2(jb|kc) − (jc|kb)] b_ck
      end do
    end do
  end do
end do
```

The fact that the doubles amplitudes of CC2 are determined by the singles amplitudes through Eqs. (92) and (93) and reduce for $t_{\mu_1} \rightarrow t^{(1)}_{\mu_1} = 0$ to the first-order amplitudes of MP2, opens a simple possibility to implement CIS(D_∞) and CIS(D) as approximations to CC2. Considering the effective Jacoby matrix, Eq. (96), as a functional of the singles amplitudes $\mathbf{A}^{eff}(t_{\mu_1}, \omega)$ one obtains the connection:

$$\text{CC2} \quad : \quad \sum_{\nu_1} \mathbf{A}^{eff}_{\mu_1\nu_1}(t^{\mathrm{CC2}}_{\kappa_1}, \omega) E_{\nu_1} = \omega E_{\mu_1}$$

$$\text{CIS(D}_\infty\text{)} \quad : \quad \sum_{\nu_1} \mathbf{A}^{eff}_{\mu_1\nu_1}(t^{(1)}_{\kappa_1}, \omega) E_{\nu_1} = \omega E_{\mu_1}$$

$$\text{CIS(D)} \quad : \quad \omega^{\mathrm{CIS(D)}} = \sum_{\mu_1\nu_1} E^{\mathrm{CIS}}_{\mu_1} \mathbf{A}^{eff}_{\mu_1\nu_1}(t^{(1)}_{\kappa_1}, \omega) E^{\mathrm{CIS}}_{\nu_1}$$

The attentive reader has probably observed that the partitioned, doubles amplitude-direct formulation for second order methods—although it removes the need to store complete sets of any doubles amplitudes—does alone not reduce much the storage requirements of these methods: the calculation of the doubles amplitudes requires the electron repulsion integrals (ERIs) in the (modified) MO basis, which are obtained through four-index transformations from the AO integrals, as e.g. in Eqs. (93) and (99). Efficient implementations of such transformations require the storage of an array with half-transformed integrals of the size of $\frac{1}{2}O^2N^2$, where O is the number of occupied and N the number of atomic orbitals, which is even slightly more than needed for the doubles amplitudes. For CC2 and also for the other second order methods for excited states and in the calculation of gradients for the MP2 energies, the doubles amplitudes need to be contracted in addition with two-electron integrals with three occupied or virtual indices, $(ai|jk)$ and $(ai|bc)$, which within the schemes sketched above would give rise to even larger storage requirements. The problem can be solved with the resolution-of-the-identity approximation for electron repulsion integrals.

7 The Resolution-of-the-Identity Approximation for ERIs

The main idea behind the resolution-of-the-identity approximation[51–58] for electron repulsion integrals can be sketched as follows: With increasing atomic orbital basis sets the products of AOs appearing for the electrons 1 and 2 in the expression for the four-index two-electron integrals,

$$(\alpha\beta|\gamma\delta) = \int_{\mathbb{R}^3}\int_{\mathbb{R}^3} \chi_\alpha(\vec{r}_1)\chi_\beta(\vec{r}_1)\frac{1}{r_{12}}\chi_\gamma(\vec{r}_2)\chi_\delta(\vec{r}_2)d\tau_1 d\tau_2 \;, \tag{100}$$

will soon become (numerically) highly linear dependent and thus it should be possible to expand these products which good accuracy in a basis set of auxiliary functions Q,

$$\chi_\alpha(\vec{r}_1)\chi_\beta(\vec{r}_1) \approx \sum_Q Q(\vec{r}_1) c_{Q,\alpha\beta} \tag{101}$$

with a dimension much smaller then that of the original product space, $N(N+1)/2$, as illustrated in Fig. 1 for an atom with only s-type functions. The coefficients $c_{Q,\alpha\beta}$ can be determined through a least square procedure. Defining the remaining error in the expansion of an orbital pair

$$R_{\alpha\beta}(\vec{r}_1) = \chi_\alpha(\vec{r}_1)\chi_\beta(\vec{r}_1) - \sum_Q Q(\vec{r}_1) c_{Q,\alpha\beta} \;, \tag{102}$$

the quadratic error in the coulomb repulsion integrals $(\alpha\beta|\gamma\delta)$ can be written as

$$(R_{\alpha\beta}|R_{\gamma\delta}) = \int_{\mathbb{R}^3}\int_{\mathbb{R}^3} R_{\alpha\beta}(\vec{r}_1)\frac{1}{r_{12}}R_{\gamma\delta}(\vec{r}_2)d\tau_1 d\tau_2 \tag{103}$$

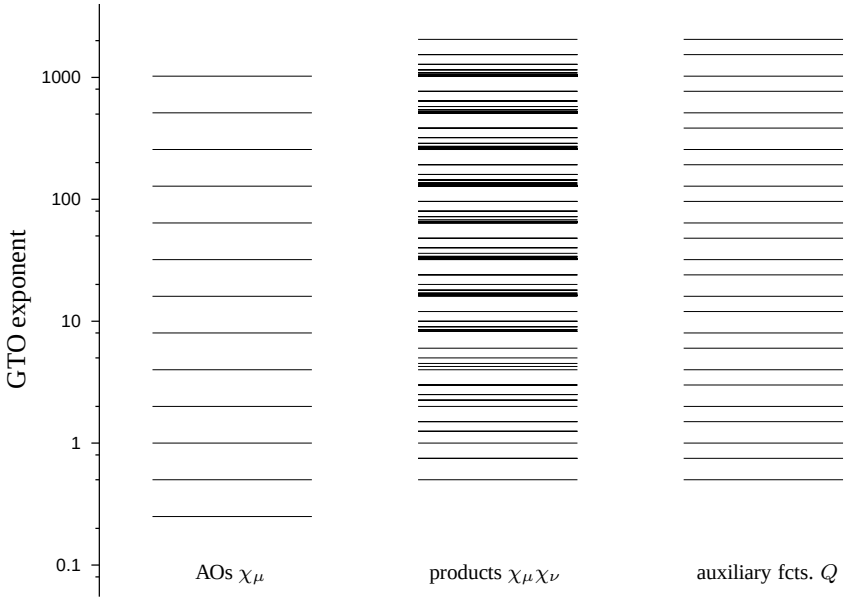

Figure 1. The left column shows exponents α_μ of an even-tempered (13s) atomic Gaussian type orbital (GTO) basis $\chi_\mu(r) = \exp(-r^2\alpha_\mu)$ and the column in the middle the exponents of all 169 overlap Gaussian functions resulting on the same atom from the products $\chi_\mu\chi_\nu$. The right column shows the exponents of an even-tempered (25s) auxiliary basis $Q(r) = \exp(-r^2\alpha_Q)$ set which could be used to expand these products.

and fulfill the Schwartz inequality

$$(R_{\alpha\beta}|R_{\gamma\delta}) \leq \sqrt{(R_{\alpha\beta}|R_{\alpha\beta})}\sqrt{(R_{\gamma\delta}|R_{\gamma\delta})}\,. \tag{104}$$

Minimization of $(R_{\alpha\beta}|R_{\alpha\beta})$ with respect to the expansion coefficients c leads to the linear equation:

$$\frac{d}{dc_{Q,\alpha\beta}}(R_{\alpha\beta}|R_{\alpha\beta}) = 0 \quad \Leftrightarrow \quad (R_{\alpha\beta}|Q) = 0 \quad \Leftrightarrow \quad (\alpha\beta|Q) - \sum_P c_{P,\alpha\beta}(P|Q) = 0 \tag{105}$$

with

$$(P|Q) = \int_{\mathbb{R}^3}\int_{\mathbb{R}^3} P(\vec{r}_1)\frac{1}{r_{12}}Q(\vec{r}_2)d\tau_1 d\tau_2\,, \tag{106}$$

$$(\alpha\beta|Q) = \int_{\mathbb{R}^3}\int_{\mathbb{R}^3} \chi_\alpha(\vec{r}_1)\chi_\beta(\vec{r}_1)\frac{1}{r_{12}}Q(\vec{r}_2)d\tau_1 d\tau_2\,. \tag{107}$$

Arranging the two-center integrals in a matrix $V_{PQ} = (P|Q)$ the expansion coefficients can be expressed as

$$c_{Q,\alpha\beta} = \sum_P (\alpha\beta|P)[V^{-1}]_{PQ}\,, \tag{108}$$

and one obtains for the four-index coulomb integrals the approximation

$$(\alpha\beta|\gamma\delta) \approx \sum_{QP} (\alpha\beta|Q)[V^{-1}]_{QP}(P|\gamma\delta) \; . \tag{109}$$

We have above derived Eq. (109) as result of a least square fitting procedure for the overlap densities $\chi_\alpha(\vec{r})\chi_\beta(\vec{r})$, which is why this approximation is also known as "density fitting"[19,20]. Eq. (109) can be compared with the expression for an (approximate) resolution of the identity for square integrable functions in three-dimensional space,

$$\mathbf{1} \approx \sum_{QP} |Q\rangle [S^{-1}]_{QP} \langle P| \qquad \text{with} \quad S_{PQ} = \int_{\mathbb{R}^3} Q(\vec{r})P(\vec{r})d\tau \; , \tag{110}$$

applied to four-center overlap integrals

$$\int_{\mathbb{R}^3} \chi_\alpha(\vec{r})\chi_\beta(\vec{r})\chi_\gamma(\vec{r})\chi_\delta(\vec{r})d\tau = \langle \alpha\beta|\delta\gamma\rangle \approx \sum_{QP} \langle \alpha\beta|Q\rangle [S^{-1}]_{QP} \langle P|\delta\gamma\rangle \; . \tag{111}$$

We see that Eq. (109) can alternatively be viewed as an (approximate) resolution of the identity in a Hilbert space where the coulomb operator $1/r_{12}$ is used to define the scalar product as in Eqs. (100) and (103). This approximation has thus all properties expected from a resolution-of-the-identity or basis set approximation as e.g. that the norm of the error in the expansion $||R_{\alpha\beta}|| = (R_{\alpha\beta}|R_{\alpha\beta})$ will always decrease with an extension of the auxiliary basis and that the approximation becomes exact in the limit of a complete auxiliary basis set $\{Q\}$.

It is important to note that the resolution-of-the-identity approximation does not—or at least not in general—reduce the computational costs for the calculation of AO four-index electron repulsion integrals, since the right hand side of Eq. (109) is more complicated to evaluate than the left hand side. A reduction of the computational costs is only achieved if the decomposition of the four-index integrals into three- and two-index intermediates, provided by this approximation, can be exploited to simplify contractions of the AO coulomb integrals with other intermediates.

A common bottleneck of all second order correlation methods (for ground and excited states) is the four-index transformation of the AO ERIs $(\alpha\beta|\gamma\delta)$ to ERIs in a molecular orbital basis (possibly modified as in Eq. (93) or (99)) with two occupied and two virtual indices:

$$(ai|bj) = \sum_\alpha C_{\alpha a} \sum_\gamma C_{\gamma b} \sum_\beta C_{\beta i} \sum_\delta C_{\delta j} \; (\alpha\beta|\gamma\delta) \; . \tag{112}$$

Efficient algorithms for this transformation require a number of floating point multiplications that scales for the individual partial transformations with $\frac{1}{2}ON^4 + \frac{1}{2}O^2N^3 + \frac{1}{2}O^2VN^2 + \frac{1}{2}O^2V^2N$ (ignoring possible sparsities in the integrals or coefficients) and, as already pointed out above, disc space in the order of $\frac{1}{2}O^2N^2$.

Using the resolution-of-the-identity approximation, the four-index integrals in the MO basis can be obtained as

$$(ai|bj) \approx \sum_P B_{P,ai} B_{P,bj} \tag{113}$$

Table 1. Comparison of elapsed wall-clock timings for RI-MP2 vs. conventional integral-direct MP2 energy calculations (# fcts. is the number of basis functions and # e^- the number of correlated electrons, T_{MP2} timings obtained with the `mpgrad` code of the TURBOMOLE package[61]).

molecule	basis	# fcts.	# e^-	T_{MP2}	T_{RI-MP2}
benzene[a]	QZVPP	522	30	28 min	24 sec
benzene[a]	aug-cc-pVTZ	756	30	3.8 h	1.2 min
$Fe(CO)_5$[a]	QZVPP	670	66	11.3 h	8.7 min
$Fe(C_5H_5)_2$[a]	QZVPP	970	66	843 h	45 min
C_{60}[a,b]	cc-pVTZ	1800	240	112 h	171 min
Calix[4]arene[b,c]	cc-pVTZ	1528	184	39.3 h	5.6 h

[a] RI-MP2 timings for `ricc2` code of the TURBOMOLE package[61]; [b] from Ref. 62;
[c] RI-MP2 timings for `rimp2` code of the TURBOMOLE package[61];

with

$$B_{P,ai} = \sum_Q [V^{-1/2}]_{PQ} \sum_\alpha C_{\alpha a} \sum_\beta C_{\beta i} (Q|\alpha\beta) \tag{114}$$

which requires only $ON^2N_x + OVNN_x + OVN_x^2 + \frac{1}{2}O^2V^2N_x$ floating point multiplications and memory or disc space in the order ONN_x. With auxiliary basis sets optimized[56,59,60] for the application in second order methods N_x is typically 2–4 $\times N_x$. Assuming that $O \ll V \approx N$ (usually given in correlated calculations), one finds that the number of floating point operations is by the RI approximation reduced by a factor of $\approx (N/O + 3)N/N_x$. With doubly polarized or correlation-consistent triple-ζ basis sets (e.g. TZVPP or cc-pVTZ) as often used with MP2 or CC2, the RI approximation typically reduces the CPU time for the calculation of the $(ai|bj)$ integrals by more than an order of magnitude. Some typical examples for MP2 calculations for the ground state correlation energy are given in Table 1. These also demonstrate how the reduction in CPU time obtained with the RI approximation increases with the size of the orbital basis set. An important point for calculations on weakly bonded (i.e. hydrogen-bridged or van der Waals) systems is that the efficiency of the integral prescreening, which is important for the performance of conventional implementations using 4-index AO ERIs, diminishes if diffuse functions are included in the basis set. For weakly bonded complexes such diffuse functions are, however, needed for an accurate description of the long range electrostatic, exchange-correlation, and dispersion interactions. As seen at the calculations for benzene with the QZVPP and the aug-cc-pVQZ basis, RI-MP2 calculations are much less sensitive to such effects: while the CPU time for the conventional MP2 calculation increases from QZVPP to aug-cc-pVQZ by more than a factor of 8, the CPU time needed for the RI-MP2 calculation increases only by a factor of 3.

However, for large scale applications at least as important is that the scaling of the storage requirements in the calculation of the integrals $(ai|bj)$ with the system size is reduced to $\mathcal{O}(ONN_x)$. In combination with the doubles amplitude-direct formulation outlined in the previous subsection, the RI approximation completely removes the need to store any intermediates larger than $\mathcal{O}(ONN_x)$ on disc or in memory. For

example the MP2 ground state energy can now be calculated using the following algorithm:

precompute $B_{Q,ai}$
do i = 1, nocc
  do j = i, nocc
    $I^{ij}_{ab} = \sum_Q B_{Q,ai} B_{Q,bj} \quad \forall \; a,b$ (matrix-matrix multiply)
    do a = 1, nvirt
      do b = 1, nvirt
        $t^{ij}_{ab} = I^{ij}_{ab}/(\epsilon_i - \epsilon_a + \epsilon_j - \epsilon_b)$
        $E_{\mathrm{MP2}} = E_{\mathrm{MP2}} + (2-\delta_{ij})\{2I^{ij}_{ab} - I^{ij}_{ba}\}t^{ij}_{ab}$
      end do
    end do
  end do
end do

The reductions are even larger for CC2 and other second order methods for excited states and for the $\mathcal{O}(\mathcal{N}^5)$-scaling steps in the calculation of MP2 gradients. It turns out that all contractions which involve other four-index integrals in the MO basis than those of $(ia|jb)$-type, needed in second order methods, can with the decomposition given by Eq. (109) reformulated such that an explicit calculation of the four-index MO integrals can be avoided.

Together with the reduction in the CPU time the elemination of the storage bottleneck opened the possibility to apply MP2 and CC2 to much larger systems as was feasible with conventional implementations based on four-index AO ERIs. Since the steep increase of the computational costs with the basis set size is reduced by the RI approximation from $\mathcal{O}(N^4)$ to $\mathcal{O}(N^2 N_x)$ it is also easier than before to carry out such calculations with accurate basis sets, as needed to exploit fully the accuracy of MP2, CC2 or the other second order methods.

At this point it becomes neccessary to ask what are the errors introduced by the RI approximation? As is obvious from the above discussion, the accuracy (but also the efficiency) of the RI approximation depends on the choice of the auxiliary basis sets. For a balanced treatment the auxiliary basis set should be optimized for the particular orbital basis used in the calculation. Firstly, because the orbital products that need to be well represented depend strongly on the orbital basis and, secondly, because the accuracy of the approximation should increase with increasing accuracy of the orbital basis to make sure that eventually a correct basis set limit will be obtained. To fully exploit the potential of the approximation it is advantageous to further "tune" the auxiliary basis set for the integrals most important in the employed electronic structure method. For second order methods these are, as shown above, $(ai|bj)$-type integrals. The auxiliary basis functions are thus used to expand products of occupied with virtual molecular orbitals:

$$\phi_a(\vec{r})\phi_i(\vec{r}) \approx \sum_Q Q(\vec{r}) c_{Q,ai} \; . \tag{115}$$

If we consider an atom, all products will be linear combinations of Gaussian type functions centered at the atom with angular momenta up to $l_{aux} = l_{orb} + l_{occ}$, where l_{orb} is

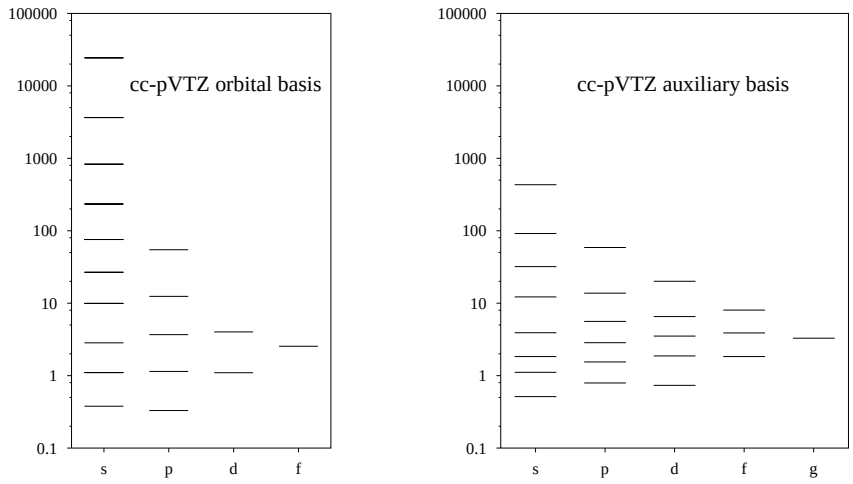

Figure 2. Exponents of the primitive GTOs in the cc-pVTZ orbital[63] (on the left) and auxiliary[59,60] (on the right) basis sets for the neon atom.

the highest angular momentum included in the orbital basis set and l_{occ} the highest angular momentum of an occupied orbital. Also the range of exponents that should be covered by the auxiliary basis can be deducted from similar considerations, but it should be taken into account that the importance of the orbital products $\phi_a\phi_i$ for electron correlation varies over orders of magnitudes. E.g., the contributions of core orbitals and similar those over very high lying tight virtual orbitals (sometimes referred to as "anti core" orbitals) is small because of large orbital energy denominators in the expression for the amplitudes. This limits the importance of tight functions in the auxiliary basis, in particular if a frozen core approximation is used and the core orbitals cannot at all contribute to the correlation treatment. In the other direction, the most diffuse exponent needed in the auxiliary basis set is bound by the exponent of any atomic orbital contributing significantly to an occupied orbital, irrespectively how diffuse functions are included in the basis set. A typical composition of an orbital basis and a respective auxiliary basis set of correlated calculations with a second order method is shown in Fig. 2 at the example of the cc-pVTZ basis sets for the neon atom.

It turns out that the above arguments, although strictly only valid for atoms, apply in practice usually also well to molecules[n]. Therefore, the auxiliary basis sets can be optimized once at the atoms for each orbital basis and then stored in a basis set library. On the TURBOMOLE web page[61] optimized auxiliary basis sets for correlated calculations with second order methods are available for several orbital basis sets including SVP[64], TZVP[65], TZVPP[56], and QZVPP[66] and most of the correlation-consistent basis sets[63,67–72] (cc-pVXZ, aug-cc-pVXZ, cc-pwCVXZ, etc.). These have been optimized[56,59,60] such that the RI error, i.e. the additional error introduced by the RI approximation, is for the

[n]An exception are the atoms with only s orbitals occupied in the ground state configuration, in particular H and Li, which in chemical bonds are often strongly polarized. For these atoms the auxiliary basis sets contain usually functions up to $l_{orb}+1$ (instead of only l_{orb}) and are often optimized on small molecules.

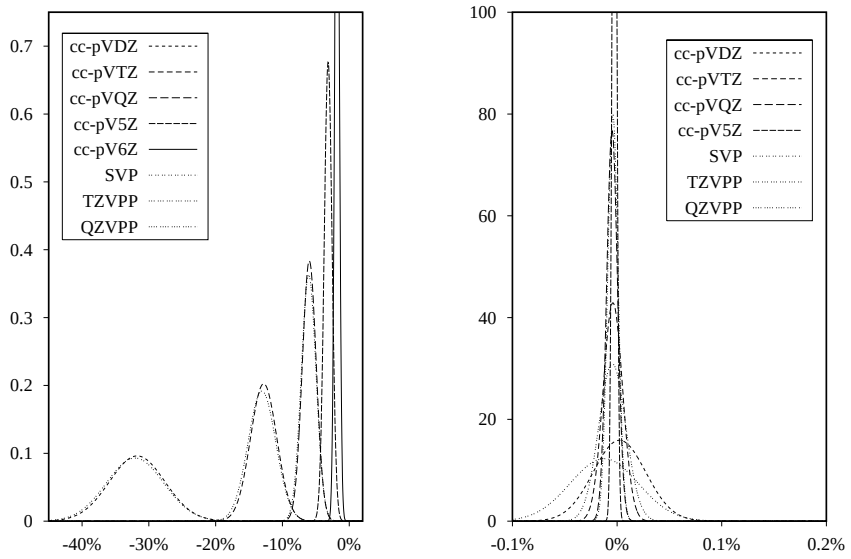

Figure 3. On the left: one-electron basis set errors in the MP2 valence correlation energy (in % of the estimated limiting value) shown as normalized Gaussian distributions determined from $\bar{\Delta}$ and Δ_{std} for a test set of 72 small and medium sized molecules with row 1 (B–Ne) and row 2 (Al–Ar) atoms[59,60]. On the right: error in the MP2 valence correlation energies due to the resolution-of-the-identity approximation for ERIs for the same test set[59,60]. Note that the scales on the abscissa differ by about three orders of magnitude!

ground state correlation energies (MP2 or CC2) about 2–3 orders of magnitudes smaller than the one-electron (orbital) basis set error of the respective orbital basis set. The correlation-consistent basis sets cc-pVXZ with X = D, T, Q, ...and the series SVP, TZVPP, QZVPP, ...constitute hierarchies that converge to the (valence) basis set limit and are thus a good example to demonstrate how orbital and auxiliary basis sets converge in parallel. Fig. 3 shows the results of an error analysis for the MP2 valence correlation energies for 72 molecules containing first and second row atoms (H, He, B–Ne, Al–Ar). The RI errors are somewhat larger for other properties than for ground state correlation energies, for which they have been optimized. In particular in response calculations for excited states the diffuse functions and also some other integral types become more important than they are for ground state calculations. But, still the RI error remains between one and two orders of magnitudes smaller than the orbital basis set error as is shown in Fig. 4 by an error analysis for RI-CC2 calculations on excited states with the aug-cc-pVTZ basis sets. Since the RI approximation is a basis set expansion approach the RI error is a smooth and usually extremely flat function of the coordinates. Therefore most of the error cancels out in the calculation of energy differences, as e.g. reaction enthalpies, and the errors in geometries are very small—typically a few 10^{-3} pm and, thus, usually below the convergence thresholds applied in geometry optimizations.

In summary, the major advantages of the resolution-of-the-identity approximation for the electron repulsion integrals for correlated second order methods are

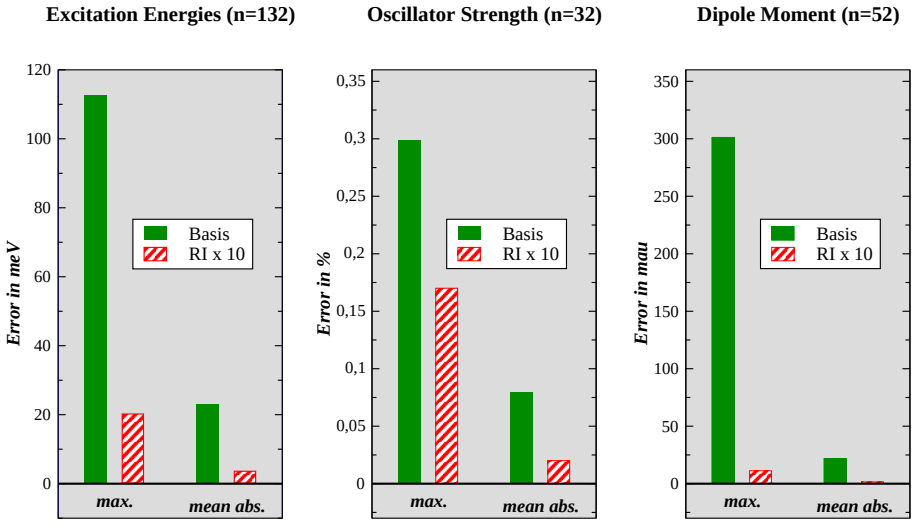

Figure 4. Mean and maximum of the one-electron orbital and the RI errors in RI-CC2 calculations for excited states with the aug-cc-pVTZ basis sets[63,69,59]. On the left: errors in excitation energies for 132 states. In the middle: errors in the oscillator strengths for 32 states. On the right: errors in the dipole moments of 52 excited states. For the test sets used and the technical details see Ref.[73], from where the data has been taken.

- It allows efficient doubles amplitude-direct implementations and eliminates the need to store any $\mathcal{O}(\mathcal{N}^4)$ arrays in memory or on disc.
- The CPU time for the correlation treatment is reduced by about an order of magnitude and more.
- It is applicable in response calculations for excited states since it does not depend on the locality of any intermediates.

Another important point related to the elimination of the huge storage demands for $\mathcal{O}(\mathcal{N}^4)$ scaling intermediates (i.e. two-electron integrals or amplitudes) is that the parallelizability of these methods is improved since less data needs to be communicated between computer nodes participating in a parallel calculation. We will come back to this point in the next section.

8 Parallel Implementation of RI-MP2 and RI-CC2 for Distributed Memory Architectures

As discussed above, the time-determining steps in RI-MP2 and other second order methods implemented with the RI approximation are the computation of the electron repulsion integrals in the MO basis $(ia|jb)$ and/or the double excitation amplitudes t_{ab}^{ij} and their contraction with integrals or other amplitudes to new intermediates, as for example

$$Y_{Q,ai} = \sum_{bj} t_{ab}^{ij} B_{Q,bj} \; . \tag{116}$$

Also for this step the computational costs increase as $\mathcal{O}(O^2V^2N_x)$. As described in Refs. 55, 73–76, $Y_{Q,ai}$ and all other intermediates calculated from t_{ab}^{ij} can efficiently be calculated in a loop over two indices for occupied orbitals with $\mathcal{O}(\mathcal{N}^2)$ memory demands. The time-determining steps of RI-MP2 can thus efficiently parallelized over pairs of indices for occupied orbitals since these are common to all steps scaling with $\mathcal{O}(O^2V^2N_x)$ or $\mathcal{O}(O^2V^3)$. An alternative could be pairs of virtual orbitals, but this would result in short loop lengths and diminished efficiency for medium sized molecules. A parallelization over auxiliary basis functions would require the communication of 4-index MO integrals between computer nodes, which would require high-performance networks. Such a solution would restrict the applicability of the program to high-end supercomputer architectures. TURBOMOLE, however, has been designed for low-cost PC clusters with standard networks (e.g. Fast Ethernet or Gigabit). Therefore we choose for the `ricc2` code a parallelization over pairs of occupied orbitals and accepted that this results in an implementation which will not be suited for massively parallel systems, since a good load balance between the participating CPUs will only be achieved for $O \gg n_{CPU}$ (vide infra).

A key problem for the parallelization of RI-MP2 and RI-CC2 is with this strategy the distribution of pairs of occupied orbitals (ij) over distributed memory nodes such that

a) the symmetry of $(ia|jb)$ with respect to permutation of $ia \leftrightarrow jb$ can still be exploited

b) the demands on the individual computer nodes for accessing and/or storing the three-index intermediates $B_{Q,ai}$ and $Y_{Q,ai}$ are as low as possible.

To achieve this, we partition the occupied orbitals into n_{CPU} batches $\mathcal{I}_m$ of (as much as possible) equal size, where n_{CPU} is the number of computer nodes. The pairs of batches $(\mathcal{I}_m, \mathcal{I}_{m'})$ with $m \leq m'$ can be ordered either on the upper triangle of a symmetric matrix or on block diagonal stripes as shown in Fig. 5. Now, each computer node gets assigned in a suitable way one block from of each diagonal, such that each node needs only access a minimal number of batches $\mathcal{I}_m$ of $B_{Q,ai}$ and $Y_{Q,ai}$. The minimal number of batches a node needs to access—in the following denoted as n_{blk}—increases approximately with $\sqrt{n_{CPU}}$. The calculation of these three-index ERIs $B_{Q,ai}$ would require about $\mathcal{O}(N^2N_X) + \mathcal{O}(ON^2N_X) \times n_{blk}/n_{CPU}$ floating point multiplications. Similar computational costs arise for some steps that involve $Y_{Q,ai}$ and other intermediates that follow the $\mathcal{O}(O^2N^2N_x)$-scaling construction of this intermediate. Thus, a conflict between minimization of the operation count and communication arises:

- If the three-index intermediates $B_{Q,ai}$ and $Y_{Q,ai}$ are communicated between the nodes to avoid multiple integral evaluations, the communication demands per node become relatively large, $\sim NN_x \times O/\sqrt{n_{CPU}}$.

- If the communication of three-index intermediates is avoided by evaluating on each node all integrals needed, the operation count for the steps which are in RI-MP2 and RI-CC2 the next expensive ones after the $\mathcal{O}(O^2V^2N_X)$ steps decreases only with $1/\sqrt{n_{CPU}}$.

The first option requires a high bandwidth for communication while the second option can also realized with a low bandwidth, but on the expense of a less efficient parallelization. For both ways a prerequisite for a satisfactory efficiency is that the total computational

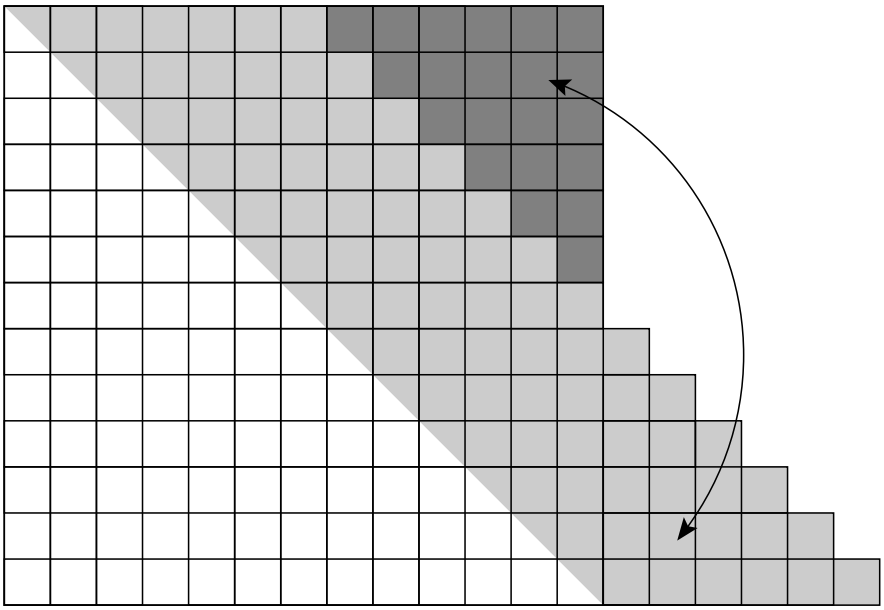

Figure 5. Arrangement of the pairs of batches $m \leq m'$ with active occupied orbitals on the upper triangle of a symmetric matrix or on block diagonal stripes.

costs are dominated by those for the $\mathcal{O}(\mathcal{N}^5)$ steps such that the time needed for multiple calculations ($\mathcal{O}(\mathcal{N}^4)$) or communication ($\mathcal{O}(\mathcal{N}^3)$) of three-index intermediates is a negligible fraction of the total time for the calculation. Both options have been realized in our parallel implementation of the `ricc2` code and shall in the following be denoted as modes for "slow communication" and "fast communication".

To implement the blocked distribution of occupied orbital indices and index pairs sketched above we define at the beginning of the calculation the following index sets:

- $\mathcal{I}_m$: a block of occupied orbitals i assigned to node m
- $\mathcal{J}_m$: merged set of the n_{blk} blocks $\mathcal{I}_n$ for which node m needs the three-index ERIs $B_{Q,ai}$ or calculates a contribution to $Y_{Q,ai}$
- $\mathcal{S}_m$: the set of all columns in the blocked distribution to which node m calculates contributions.
- $\mathcal{R}_m(n)$: the indices of the rows in column n assigned in this distribution to node m

With this concept one obtains an efficient parallelization of most program parts that involve at least one occupied index. These parts use only three- and two-index AO integrals and include all steps that scale with $\mathcal{O}(\mathcal{N}^4)$ or $\mathcal{O}(\mathcal{N}^5)$ in RI-MP2 single point calculations for energies or RI-CC2 calculations for excitation energies and spectra. For a discussion of additional demanding steps in the computation of analytic derivatives (gradients) the interested reader is referred to Refs. 55, 75–77. Here, we only sketch how the computation

of the intermediate $Y_{Q,ai}$ can be implemented without any MPI communication once each computer node has calculated or received all integral intermediates $B_{Q,ai}$ needed there:

loop $n \in \mathcal{S}_m$, loop I (where $I \subseteq \mathcal{I}_n$)

read $B_{Q,ai}$ for all $i \in I$

loop $n' \in \mathcal{R}_m(n)$, loop $j \in \mathcal{I}_{n'}$ with $j \leq i$

* read $B_{Q,bj}$
* $t_{ab}^{ij} \leftarrow B_{Q,ai} B_{Q,bj} / \left\{ \epsilon_i - \epsilon_a + \epsilon_j - \epsilon_b \right\}$
* $Y_{P,ai} \leftarrow (2t_{ab}^{ij} - t_{ba}^{ij})\ B_{P,bj}$ and for $j \neq i$ also $Y_{P,bj} \leftarrow (2t_{ab}^{ij} - t_{ba}^{ij})\ B_{P,ai}$

end loop j, loop n'

store $Y_{P,ai}$ and $Y_{P,bj}$ on disk (distributed)

end loop I, loop n

If only the RI-MP2 energy is needed, it can be evaluated directly after the calculation of the integrals $(ia|jb)$ and amplitudes t_{ab}^{ij} as described in Sec. 6.1 and the calculation of $Y_{Q,ai}$ can be skipped. If the latter intermediates are needed, the contributions to the $Y_{Q,ai}$ intermediate can be added and redistributed (after the loop over n has been closed) such that each node has the complete results for $Y_{P,ai}$ for all $i \in \mathcal{J}_m$ (requiring the communication of $\approx 2OVN_x/\sqrt{n_{CPU}}$ floating point numbers per node).

8.1 Performance for parallel RI-MP2 energy calculations

To benchmark the calculation of MP2 energies we used four typical test systems with structures as shown in Fig. 6:

- A calicheamicine model taken from Ref. 78, which has also no point group symmetry. These calculations have been done in the cc-pVTZ basis sets[63,67,68] with 934 orbital and 2429 auxiliary functions and 124 electrons have been correlated.

- The fullerene C_{60}, which has I_h symmetry, but the calculations reported here exploited only the Abelian subgroup D_{2h}. The cc-pVTZ basis set has been used, which in this case comprises 1800 orbital and 4860 auxiliary basis functions and the 240 valence electrons were correlated.

- A chlorophyll derivative which has also no point group symmetry. The cc-pVDZ basis with in total 918 orbital and 3436 auxiliary functions have been used and 264 electrons have been correlated.

- A cluster of 40 water molecules as an example for a system where integral prescreening leads to large reductions in the costs in conventional MP2 calculations. The basis sets are 6-31G$*$ for the orbital[79] and cc-pVDZ for the auxiliary[59] basis with, respectively, 760 and 3840 functions; the point group is C_1 and the 320 valence electrons have been correlated.

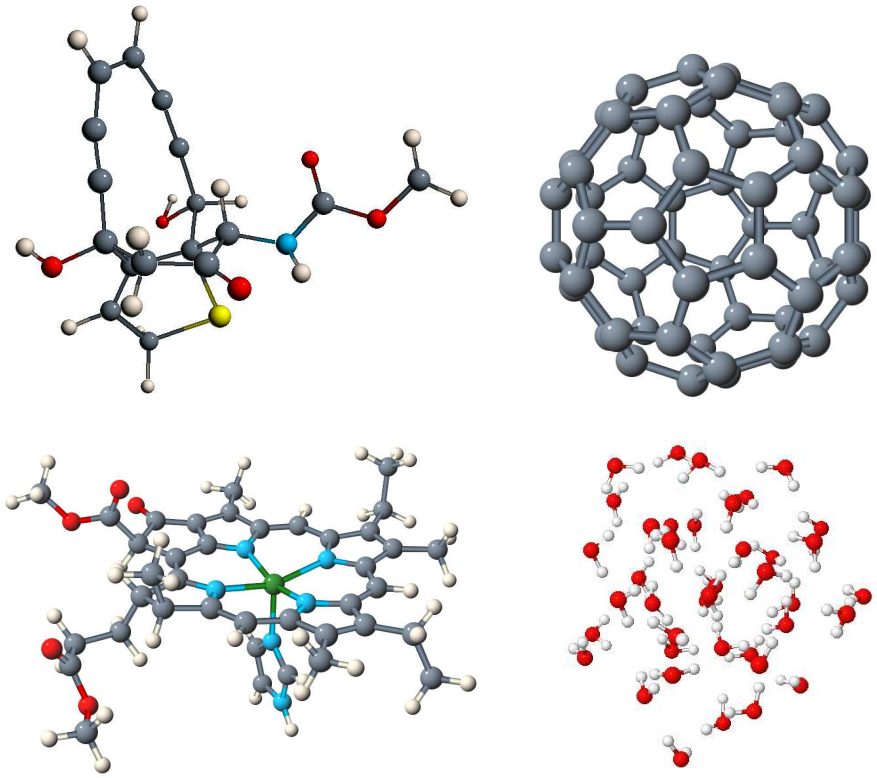

Figure 6. Structures of the four test examples used to benchmark the performance of parallel RI-MP2 calculations. For the details of the basis sets and the number of correlated electrons see text.

The maximum amount of core memory used by the program was in all calculations limited to 750 Mb. The calculations were run on two different Linux cluster: one cluster with ca. 100 Xeon Dual 2.8 GHz nodes connected through a cascaded Gigabit network and a second cluster with ca. 64 Athlon 1800MP MHz nodes connected through a 100 MBit fast Ethernet network. Due to a much larger load on the first cluster and its network the transfer rates reached in the benchmark calculations varied between ca. 80–200 MBit/sec per node. On the Athlon Cluster with the 100 MBit network we reached transfer rates of ca. 20–50 MBit/sec per node.

Fig. 7 shows timings for the calculation of MP2 energies for the C_{60} fullerene. On both architectures in sequential runs about 55% of the time are spend in the matrix multiplication for the $\mathcal{N}^5$ step. With increasing number of nodes this ratio slowly decreases. In case of the "slow communication" mode because the costs for the integral evaluation take an increasing fraction of the total wall time; in the "fast communication" mode (and here in particular on the cluster with the slower network) because of the increasing fraction of time spent in the communication of the 3-index MO integral intermediate $B_{Q,ai}$. Not parallelized steps—as e.g. the evaluation of the matrix V_{PQ} of 2-index ERIs, its Cholesky decomposition and formation of the inverse— take only a marginal fraction of the total

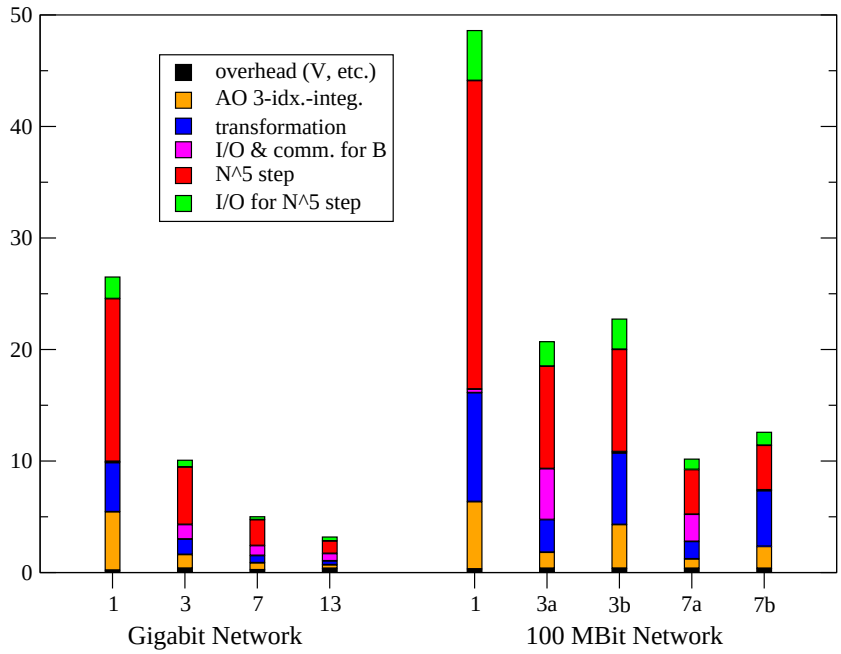

Figure 7. Timings for the most important steps in parallel RI-MP2 energy calculations for C_{60} in the cc-pVTZ basis (240 electrons correlated). For technical details of the machines used see text. At the abscissa we indicated the number of CPUs used for the calculations. For the cluster with a 100 MBit Network letters "a" and "b" are added, respectively, for calculations in the "fast" and "slow" communication modes. On the other cluster only the former program mode has been tested. The fraction denoted "overhead" includes most non-parallel steps, as the calculation of the Coulomb metric V and the inverse of its Cholesky decomposition, I/O and communication of MO coefficients, etc. With "AO 3-idx.-integ" we denoted the time spend for the calculation of the AO 3-index integrals $(P|\mu\nu)$ and with "transformation" and "I/O & comm. for B" the fractions spend in the three-index transformations for the intermediates B^i_{Qa} and for saving these intermediates on disk and/or distributing them to other computer nodes. "N^5 step" and "I/O for N^5 step" are the fractions spend, respectively, in the $\mathcal{N}^5$-scaling matrix multiplication and the I/O of B intermediates during the calculation of two-electron MO integrals. For parallel calculations idle times caused by non-perfect load-balance are included under the point "I/O for N^5 step".

wall time and the fraction of the time spend in the I/O stays approximately constant with the number of nodes used for the calculation. Another important message from Fig. 7 is, that even with a relatively slow network it is advantageous to communicate the 3-index intermediates, although on the cluster with the slower network the difference in performance between the two modes is not large. We note, however, that this depends also on the size of the system and the basis sets.

Because of the symmetry of the molecule, an RI-MP2 energy calculation for C_{60} is today not really a large scale application. The same holds for the other three test examples. Nevertheless, already for these (for parallel calculations) small examples the speed ups obtained with the present implementation are reasonable as Fig. 8 shows. The speed up obtained increases with the system size as the computational costs become dominated by the $\mathcal{N}^5$-scaling matrix multiplication in the construction of the MO 4-index ERIs and

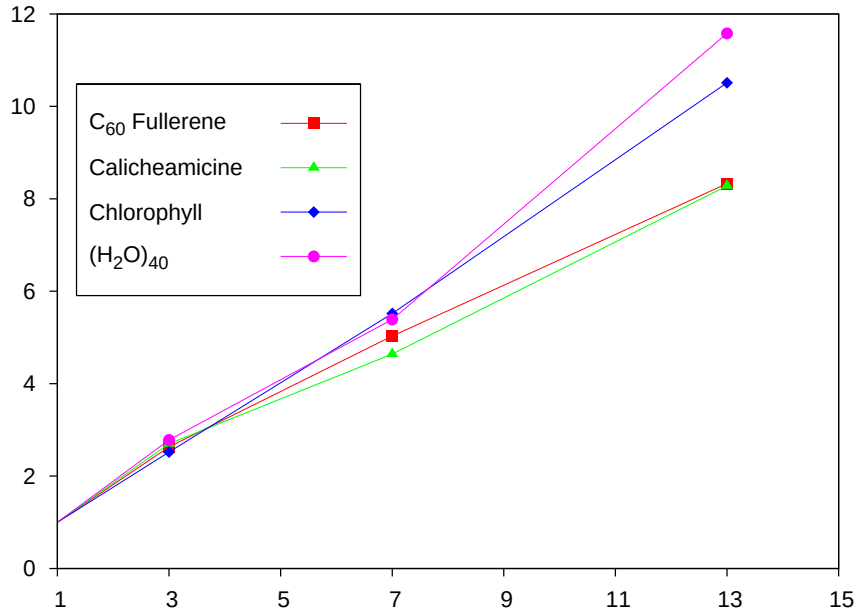

Figure 8. Speed up obtained for parallel RI-MP2 energy calculations on the Linux cluster with Gigabit network with four test examples. The number of nodes is given on the abscissa and the speed up (defined as wall time of parallel calculation dived by the wall time of the sequential run) is indicated on the ordinate.

the less good parallelizing calculation and/or communication of the 3-index MO integrals becomes unimportant for the total wall time.

9 RI-MP2 Calculations for the Fullerenes C_{60} and C_{240}

An important aspect of the parallel implementation of RI-MP2 is that it allows to combine the fast RI-MP2 approach with *parallel* Hartree-Fock self-consistent field (HF-SCF) calculations, available today in many program packages for electronic structure calculations, to optimize geometries for relatively large molecules at the MP2 level. An example for such a calculation is the determination of the MP2 basis set limit for the ground state equilibrium structure of C_{60}. The structure of C_{60} has been studied before at the MP2 level by Häser and Almlöf[81] in 1991, but due to the large computational costs of MP2 the calculations had to be limited to a singly polarized TZP basis set ([5s3p1d], 1140 basis functions), which is known to cover only about 75% of the correlation energy. With the parallel implementation of RI-MP2 it was now possible repeat this calculation using cc-pVTZ basis ([4s3p2d1f], 1800 basis functions), which gives typically correlation energies almost within 90% of the basis set limit, and the cc-pVQZ basis ([5s4p3d2f1g], 3300 basis functions), which usually cuts the remaining basis set errors again into half. The results for the bond lengths and the total energies are summarized in Table 2 together with the results from Ref. 81 and the available experimental data. As anticipated from the quality of the basis sets, the result for the correlation energy increases by about 15% from the MP2/TZP

Table 2. Equilibrium bond distances of C_{60}; d_{C-C} denotes the distance between adjacent C atoms in a five-ring and $d_{C=C}$ the distance between to the C-C bond shared between to six-rings. The bond distances are given in Ångstrøm (Å) and the total energies in Hartrees (H).

Method	d_{C-C}/Å	$d_{C=C}$/Å	Energy/hartree
SCF/DZP[a]	1.450	1.375	-2272.10290
SCF/TZP[a]	1.448	1.370	-2272.33262
MP2/DZP[b]	1.451	1.412	-2279.73496
MP2/TZP[b]	1.446	1.406	-2280.41073
MP2/cc-pVTZ[c]	1.443	1.404	-2281.65632
MP2/cc-pVQZ[c]	1.441	1.402	−2282.34442
exp.[d]	1.458(6)	1.401(10)	
exp.[e]	1.45	1.40	
exp.[f]	1.432(9)	1.388(5)	

[a] from Ref. 80; [b] from Ref. 81; [c] from Ref. 76, at the MP2/cc-pVTZ optimized structure the SCF energy is -2272.40406 hartree; [d] gas phase electron diffraction, Ref. 82; [e] solid state NMR, Ref. 83; [f] X-ray of $C_{60}(OsO_4)$(4-*tert*-butylpyridine)$_2$, Ref. 84;

to the MP2/cc-pVTZ calculation and again by about 6% from the cc-pVTZ to the cc-pVQZ basis. Also the changes in the bond lengths from the MP2/TZP to the MP2/cc-pVQZ level are with 0.004–0.005 Å of the same magnitudes as between the MP2/DZP and MP2/TZP calculations. But the difference between the two C–C distances remains almost unchanged, and also the comparison with the experimental data is not effected, since the error bars of the latter are with about ± 1 pm of the same order of magnitude as the basis set effects. The inclusion of core correlation effects would lead to a further slight contraction of the bond lengths, but the largest uncertainty comes from higher-order correlation effects which would probably increase the bond lengths in this system, but likely not more than 0.005 Å. Therefore, it is estimated that the MP2/cc-pVQZ results for the equilibrium bond distances (r_e) of the buckminster fullerene C_{60} are accurate within $\pm$ 0.005 Å. This is slightly less than the uncertainty of the presently available experimental data. Within their uncertainties the ab initio calculations and the experiments are thus in good agreement.

Another example demonstrating which system sizes can be handled with the parallel implementation of RI-MP2 is the next larger icosahedral homologue of the Buckminster fullerene C_{60}: the C_{240} molecule.The correlation consistent triple-ζ basis cc-pVTZ comprises for this molecules 7200 basis functions and, if the $1s$ core orbitals are kept frozen, 960 electrons have to be correlated. This calculation has been run on a Linux cluster with Dual Xeon 2.8 GHz nodes connected by a Gigabit network. Because the memory demands of implementation increase for non-Abelian point groups with the square of the dimension of the irreducible representations the calculation was carried out in the D_{2h} subgroup of the molecular point group I_h. On 19 CPUs the RI-MP2 calculation was completed after 16 hours and 6 minutes. About 12.5% of the time was spend in the evaluation and distribution of the two- and three-index integrals and 85% in the $\mathcal{O}(O^2V^2N_x)$ scaling construction of

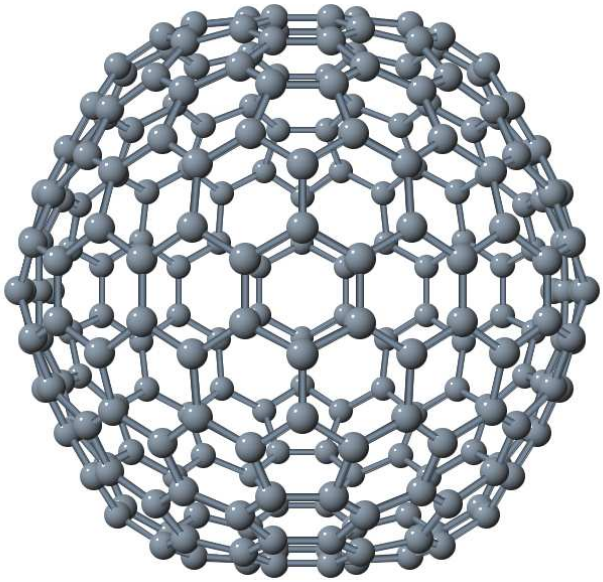

Figure 9. Structure of the icosahedral fullerene C_{240}.

the four-index integrals in the MO basis $(ia|jb)$. In D_{2h} symmetry about 6×10^{11} four-index MO integrals ($\approx$ 4.8 TByte) had to be evaluated to calculate the MP2 energy. This shows that such a calculation would with a conventional (non-RI) MP2 require either an enormous amount of disc space or many costly re-evaluations of the four-index AO two-electron integrals and would thus even on a massively parallel architecture difficult to carry out. To the best of our knowledge this is the largest canonical MP2 calculation done until today. With the parallel implementation of the RI-MP2 approach calculations of this size can now be carried out on PC clusters build with standard (and thus low cost) hardware and are expected to become soon routine applications.

The total energy of C_{240} obtained with MP2/cc-pVTZ at the BP86[85–87]/SVP[64,58] optimized structure[88] is -9128.832558 H. For the buckminster fullerene C_{60} a single point MP2/cc-pVTZ calculation at the BP86/SVP optimized geometry gives a total energy of -2281.645107 H. Neglecting differential zero-point energy effects, which in this case are expected to be small, we obtain from our calculations an estimate for the reaction enthalpy of $4 \times C_{60} \rightarrow C_{240}$ of -2.25 H, i.e. a change in the enthalpy of formation per carbon atom of -9.4 mH or -25 kJ/mol. This can be compared with the experimental result[89] for $\Delta_f H^0$ of C_{60} relative to graphite of 39.25 ± 0.25 kJ/mol. Thus, the present calculations predict that the strain energy per carbon atom in C_{240} is with $\approx$ 15 kJ/mol only about 35% of the respective value in C_{60}.

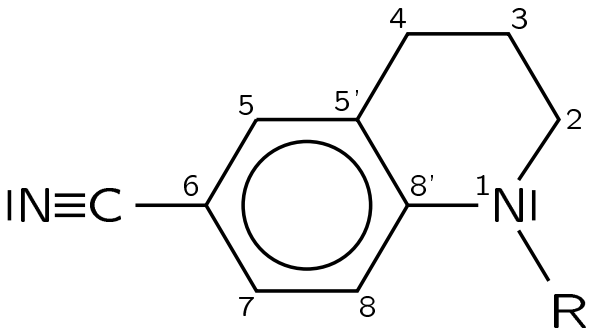

Figure 10. Enumeration of the atoms in NMC6 (R = methyl) and NTC6 (R = *tert*butyl). For DMABN R = methyl and aliphatic six-ring is replaced by a (second) methyl group at the N-atom.

10 Geometry Optimizations for Excited States with RI-CC2: The Intramolecular Charge Transfer States in Aminobenzonitrile Derivatives

An example for the optimization of excited state equilibrium structures with RI-CC2 are recent investigations[90,91] on N-alkyl-substituted aminobenzonitriles (see Fig. 10). A problem discussed for this class of molecules in the literature since several decades in many publications has been the structure of a so-called intramolecular charge-transfer (ICT) state which is observed in fluorescence and femtosecond spectroscopic experiments close to a so-called locally excited (LE) state.[92–96] The two states belong to the two lowest singlet hypersurfaces S1 and S2, which are connected through a conical intersection seam. Experimental and theoretical results[97–101] indicate that the reaction coordinate which connects the minima on the two surfaces through the conical intersection involves a Kekulé-like distortion of the phenyl ring and a twist of the amino group, which for the N,N-dimethylaminobenzonitrile (DMABN) is known to be in the ground state almost coplanar with the phenyl ring. That the twisting coordinate is involved probably explains distinct effects of different aliphatic substituents at the amino group on the fluorescence properties (vide infra) which are intensively discussed in the literature. In 1-*tert*-butyl-6-cyano-1,2,3,4-tetrahydroquinoline (NTC6) and 1-metyl-6-cyano-1,2,3,4-tetrahydroquinoline (NMC6) a twist of the amino group is restricted by the aliphatic ring to a certain range of torsion angles, but on the other side the sterically demanding bulky *tert*-butyl substituent in NTC6 disfavors a coplanar orientation. CC2/TZVPP calculations[91] predict for the ground state of NMC6 an almost coplanar orientation of the phenyl and amino moieties, but for NTC6 a tilted geometry with a twist angle of about 28° (cmp. Table 3).

Table 4 gives an overview on the CC2/TZVPP results for some spectroscopic properties of DMABN, NMC6 and NTC6, e.g. the absorption and emission energies and the dipole moments in comparison with the available experimental data. For the ICT states we found for NMC6 and NTC6 three conformations. Table 5 summarizes the results for the energetically lowest-lying structures and the ones with the highest dipole moments denoted as, respectively, ICT-1 and ICT-2, in comparison with the structure of the single conformer in the ICT state of DMABN. In all three molecules the ICT equilibrium geometries display

Table 3. Calculated bond lengths (pm) and angles (°) of the ground states of DMABN, NMC6, and NTC6 in comparison (from Ref. 91, for the enumeration of the atoms see Fig. 10).

	DMABN	NMC6	NTC6
d(C_{Ph}-N_1)[a]	137.7	138.1	139.0
d($C_8C_{8'}$)	141.4	141.2	141.2
d($C_{8'}C_{5'}$)	141.4	141.9	141.1
d(C_7C_8)	138.7	138.7	138.9
d($C_5C_{5'}$)	138.7	138.9	138.6
d(C_6C_7)	140.2	140.0	139.9
d(C_5C_6)	140.2	140.2	140.3
d(C_6C_{CN})	142.7	142.6	142.6
d(CN)	118.2	118.1	118.1
τ[b]	0	0.1	27.9
ϕ_1[c]	23	24.8	18.9
ϕ_2[d]	< 1	1	1.5

[a] bond distance between phenyl ring and amino group. [b] torsion angle, defined as dihedral angle of the normals defined by the planes C_8-$C_{8'}$-$C_{5'}$ and C_2-N_1-C_R and the bond $C_{8'}$-N_1. [c] out-of-plane angle of the bond $C_{8'}$-N_1 with respect to the plane C_2-N_1-C_R ("wagging" angle). [d] out-of-plane angle of the bond $C_{8'}$-N_1 with respect to the plane C_8-$C_{8'}$-C_5.

marked quinoid distortions of the aromatic ring system. An important finding, which was not anticipated from the experimental data that has been available in the literature, is that the aromatic ring is no longer confined to planarity in the excited state. Rather, the carbon atom labeled 8' in Fig. 10 is pyramidalized. Therefore the aliphatic six-ring can accommodate twist angles of the amino group of up to 60–70°, as illustrated in Fig. 11, and in this way energetically low-lying twisted ICT states can be realized even in NTC6 and NMC6. In the literature it was before assumed that the aliphatic six-ring, which connects the amino group with the phenyl ring restricts these molecules to "planarized" structures and makes such a twist impossible.

The transition to the ICT state is at the ground state geometry dominated by the one-electron HOMO→LUMO excitation in these molecules. Both orbitals are of Ph-N antibinding character, but the orbital energy of the LUMO decreases slightly faster with increasing twisting angle than the energy of the HOMO and already such a simple model predicts for the ICT state close to the ground state geometry a gradient directed to a twisted structure. With increasing twisting angle the transition assumes an increasing contribution from the HOMO-2→LUMO excitation. The HOMO-2 is the Ph-N binding counterpart of the HOMO and increases in energy with the twisting angle and mixes with the HOMO. As the angle approaches 90° one of the two orbitals becomes the lone-pair at the amino N-atom while the other is localized in the aromatic system and the transition to the ICT state is dominated by the $n \rightarrow \pi^\star$ excitation. In a many electron picture this change in the character of the excitation corresponds to an avoided crossing of S2 with another, at

Table 4. Calculated absorption and emission energies and dipole moments for DMABN, NMC6 and NTC6 in comparison with experimental data. The CC2 results for absorption and emission energies are vertical electronic transition energies; the dipole moments were calculated as analytic derivatives of the CC2 total energies.

	DMABN		NMC6		NTC6	
	CC2[a]	exp.	CC2[a]	exp.	CC2[a]	exp.
absorption (S_1) [eV]	4.41[b]	4.25[c]	4.31[d]		4.33[d]	
absorption (S_2) [eV]	4.77[b]	4.56[c]	4.58[d]	4.32[e]	4.43[d]	4.14[e]
osc. strengths (S_1)	0.03[bf]		0.03[f]		0.03[f]	
osc. strengths (S_2)	0.62[bf]		0.49[f]		0.51[f]	
T_e (LE) [eV]	4.14		4.07		3.91	
emission (LE) [eV]	3.78[g]	3.76[h]	3.67[g]	3.67[e]	3.34[g]	3.50[e]
T_e (ICT) [eV]	4.06–4.16[i]		4.18		3.71	
emission (ICT) [eV]	2.49–3.27[ig]	2.8–3.2[j]	2.53[gk]		2.51[gk]	2.8[l]–3.3[e]
dipole (GS) [D]	7.4	6.6[j]	7.5	6.8[m]	7.7	6.8[m]
dipole (LE) [D]	10.1	9.7[j]	10.4	10.6[m]	12.6	
dipole (ICT) [D]	13.3–15.1[i]	17 ± 1[j]	12.7[k]		13.5[k]	17–19[m]

[a] Unless otherwise indicated the CC2 results for DMABN are taken from Ref. 90 and those for NMC6 and NTC6 from Ref. 91. [b] CC2/TZVPP (Ref.[102]). [c] EELS band maximum (Ref. 103). [d] Vertical excitation energy to the L_a (or S_2) state which has a significantly larger oscillator strength. [e] Experimental band maximum in n-hexane (Ref. 94). [f] Oscillator strength for vertical electronic transition calculated at the CC2/TZVPP level in length gauge. [g] Vertical energy separation from ground state at the excited state equilibrium structure. [h] Maximum of dispersed emission from jet-cooled DMABN (Ref. 104). [i] The first value is the result for the gas phase equilibrium structure and the second value is obtained at the C_{2v} symmetric saddle point (Ref. 90). [j] Emission energy from ICT state from maxima of fluorescence bands; ground state dipole moment derived from the dielectric constant and refractive index in dioxane and the excited state dipole moments from time-resolved microwave conductivity measurements in dioxane (Ref. 105). [k] Value refers to the ICT-2 conformer. [l] Experimental band maximum in methanol (Ref. 94). [m] Derived from solvatochromic shift of fluorescence maximum (Ref. 94).

the ground state structure energetically higher lying, charge-transfer state—in DMABN according to DFT/SCI calculation in Ref. 106 the S5 state. The avoided crossing with this state is the main driving force for the formation of the TICT structures (twisting and pyramidilization at the $C_{8'}$ atom) in DMABN, NTC6, NMC6 and other alkyl-substituted amino-benzonitrils. It leads to a pronounced stabilization of the ICT state at large twisting angles and enhances the charge-transfer character, as it is apparent from the expectation values for the dipole moment (see Table 4). For all three molecules, DMABN, NMC6, and NTC6, one finds a similar change in the electronic character from the vertical excitation in the Franck-Condon region to the equilibrium geometries of the ICT states. This is in line with the interpretation of recent measurements of the short-time dynamics in DMABN derivatives after excitation to S2.[97,107–110]

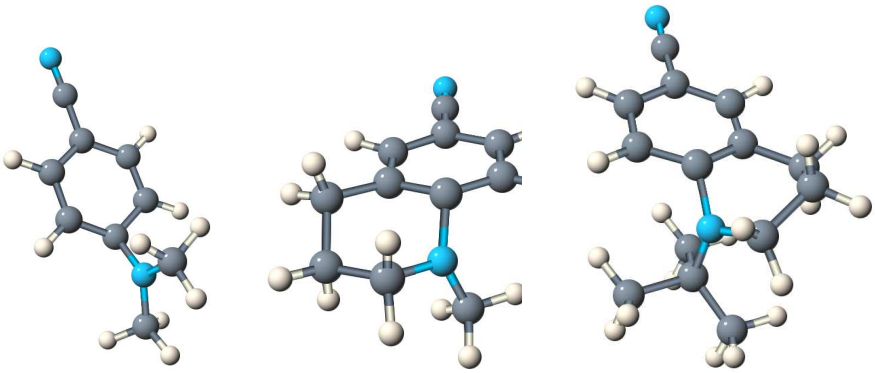

Figure 11. Equilibrium structures of the ICT states in DMABN, NMC6, and NTC6.

For NTC6 the increase in the twist angle from the ground to the excited ICT states reduces the steric strain of the *tert*-butyl group und thus compensates for the hindrance of the twist by the aliphatic bridge. We obtain at the CC2/TZVPP level that for NTC6 and DMABN the ICT states are energetically slightly below the LE state, which is reached by an one-electron transition from the PH-N antibinding HOMO to a Ph-N non-binding orbital. For NMC6, however, the inhibition of a 90° twist is not compensated by the release of a similar strain since the methyl substituent is sterically much less demanding. Thus, in difference to DMABN and NTC6 the LE→ICT reaction for NMC6 is predicted by the RI-CC2 calculations to be slightly endotherm. This explains why NMC6 is not dual fluorescent, in contrast to DMABN and NTC6.

11 Summary

The computational costs of wavefunction based correlated ab initio methods that treat the electron–electron interaction correctly through second order (so-called second order or approximate doubles methods) have in conventional implementations been dominated by the huge operation counts for the calculation of the four-index electron repulsion integrals in the AO basis and their transformation to the MO basis. The costs for these steps increase rapidly with the size of the system studied and the basis sets used. In addition, also the huge storage demands for the four-index transformation hindered applications on large systems.

With the resolution-of-the-identity approximation for the electron repulsion integrals the CPU time for the calculation of the MO integrals needed in second order methods is reduced by about an order of magnitude (and sometimes even much more) and the scaling of the storage demands is reduced from $\mathcal{O}(O^2N^2)$ to $\mathcal{O}(OVN_x)$. If optimized auxiliary basis sets are used, as they today are available for many orbital basis sets, the errors due to RI approximation are insignificant compared to the errors due to the incompleteness of the orbital basis sets.

In combination with a new parallel implementation in TURBOMOLE for distributed memory architectures (e.g. PC clusters) it became now possible to carry out RI-MP2 calculations for energies and structures with several thousands of basis functions and several

Table 5. Calculated bond lengths (pm) and angles (°) and weights of the two most important one-electron excitations (%) for the intramolecular charge-transfer states of DMABN, NMC6, and NTC6 in comparison (from Ref. 91, for the enumeration of the atoms see Fig. 10).

	DMABN	NMC6		NTC6	
	ICT	ICT-1	ICT-2	ICT-1	ICT-2
d(C_{Ph}-N_1)[a]	144.3	146.8	145.0	146.8	145.7
d($C_8C_{8'}$)	144.6	143.5	144.8	142.9	144.9
d($C_{8'}C_{5'}$)	144.6	146.2	144.5	146.0	143.6
d(C_7C_8)	137.2	137.2	137.7	137.3	137.8
d($C_5C_{5'}$)	137.2	138.0	136.9	137.9	137.1
d(C_6C_7)	142.9	143.4	142.4	143.8	142.4
d(C_5C_6)	142.9	141.8	143.7	141.9	144.0
d(C_6C_{CN})	140.9	141.2	140.9	141.1	140.8
d(CN)	118.9	118.8	118.9	118.8	118.9
τ[b]	90	54.3	66.6	58.5	65.0
ϕ_1[b]	0	24.1	14.7	20.7	5.2
ϕ_2[b]	41	43.9	44.6	36.4	43.4
HOMO→LUMO		65	62	69	64
HOMO-2→LUMO		15	17	25	16

[a] bond distance between phenyl ring and amino group. [b] for the definition of the torsion and the out-of-plane angles see Table 3.

hundreds of correlated electrons. This extends the applicability of MP2 to systems which else can only be treated with SCF or DFT methods. Calculations on excited states using e.g. the approximate coupled-cluster singles and doubles method CC2 or the perturbative doubles correction to configuration interaction singles, CIS(D), are somewhat more involved and structure optimizations for excited states are (because of weakly avoided crossings or conical intersections) much less straightforward than for ground states. With the parallel implementation of RI-CC2 they become still feasible for molecules with more than 30 atoms and many hundred basis functions even if the molecular structure has no point group symmetry.

Acknowledgments

The author in indebted to A. Köhn and A. Hellweg for their contributions to the RICC2 program and to the calculations reviewed in this manuscript. Financial support by the Deutsche Forschungsgemeinschaft (DFG) for the reported work is gratefully acknowledged.

References

1. P. Pulay. *Chem. Phys. Lett.*, 100:151–154, 1983.
2. M. Schütz, G. Hetzer, and H.-J. Werner. *J. Chem. Phys.*, 111:5691–5705, 1999.
3. G. Hetzer, M. Schütz, H. Stoll, and H. J. Werner. *J. Chem. Phys.*, 113:9443–9455, 2000.
4. G. E. Scuseria and P. Y. Ayala. *J. Chem. Phys.*, 111:8330–8343, 1999.
5. P. E. Maslen and M. Head-Gordon. *J. Chem. Phys.*, 109:7093–7099, 1998.
6. S. H. Li, J. Ma, and Y. S. Jiang. *J. Comp. Chem.*, 23:237–244, 2002.
7. K. Morokuma. *Philosophical Transactions of the Royal Society of London Series A – Mathematical Physical and Engineering Sciences*, 360:1149–1164, 2002.
8. M. Schütz and H. J. Werner. *J. Chem. Phys.*, 114:661–681, 2001.
9. M. Schütz. *Phys. Chem. Chem. Phys.*, 4:3941–3947, 1993.
10. S. Sæbo and P. Pulay. *J. Chem. Phys.*, 87:3975–3983, 2001.
11. D. S. Lambrecht and C. Ochsenfeld. *J. Chem. Phys.*, 123:184102, 2005.
12. S. Grimme. *J. Chem. Phys.*, 118:9095–9102, 2003.
13. S. Grimme. *J. Comput. Chem.*, 24:1529–1537, 2003.
14. Y. S. Jung, R. C. Lochan, A. D. Dutoi, and M. Head-Gordon. *J. Chem. Phys.*, 121:9793–9802, 2004.
15. R. C. Lochan, Y. S. Jung, and M. Head-Gordon. *J. Phys. Chem. A*, 109:7598–7605, 2005.
16. T. D. Crawford and R. A. King. *Chem. Phys. Lett.*, 366:611–622, 2002.
17. T. Korona and H. J. Werner. *J. Chem. Phys.*, 114:3006–3019, 2003.
18. T. Korona, K. Pflüger, and H. J. Werner. *Phys. Chem. Chem. Phys.*, 6:2059–2065, 2004.
19. M. Schütz and F. R. Manby. *Phys. Chem. Chem. Phys.*, 5:3349–3358, 2003.
20. H.-J. Werner, F. R. Manby, and P. J. Knowles. *J. Chem. Phys.*, 118:8149, 2003.
21. P. Pulay. *J. Chem. Phys.*, 73:393, 1980.
22. P. Pulay. *J. Comp. Chem.*, 4:556, 1982.
23. T. Helgaker, P. Jørgensen, and J. Olsen. *Molecular Electronic-Structure Theory*. John Wiley & Sons, New York, 2000.
24. S. Grimme and M. Waletzke. *Phys. Chem. Chem. Phys.*, 2:2075–2081, 2000.
25. B. O. Roos, K. Andersson, M. P. Fülscher, P. A. Malmqvist, L. Serrano-Andres, K. Pierloot, and M. Merchan. *Advances in Quantum Chemistry*, 93:219–331, 1996.
26. J. Olsen and P. Jørgensen. *J. Chem. Phys.*, 82:3235, 1985.
27. J. Olsen and P. Jørgensen. *Time-Dependent Response Theory with Applications to Self-Consistent Field and Multiconfigurational Self-Consistent Field Wave Functions*, In D. R. Yarkony, editor, *Modern Electronic Structure Theory*, volume 2, chapter 13, pages 857–990. World Scientific, Singapore, 1995.
28. O. Christiansen, P. Jørgensen, and C. Hättig. *Int. J. Quantum Chem.*, 68:1–52, 1998.
29. C. Hättig. *Accurate Coupled Cluster Calculation of Nonlinear Optical Properties of Molecules*, In M. G. Papadopoulos, editor, *On the non-linear optical response of molecules, solids and liquids: Methods and applications*. Research Signpost, 2003.
30. P. Salek, O. Vahtras, T. Helgaker, and H. Agren. *J. Chem. Phys.*, 117:9630–9645, 2002.
31. O. Christiansen, S. Coriani, J. Gauss, C. Hättig, P. Jørgensen, F. Pawłowski, and A.

Rizzo. *Accurate NLO Properties for small molecules. Methods and results*, In M. G. Papadopoulos, J. Leszczynski, and A. J. Sadlej, editors, *Nonlinear optical properties: From molecules to condensed phases*. Kluwer Academic Publishers, London, 2006.
32. O. Christiansen, H. Koch, and P. Jørgensen. *Chem. Phys. Lett.*, 243:409–418, 1995.
33. O. Christiansen, H. Koch, P. Jørgensen, and T. Helgaker. *Chem. Phys. Lett.*, 263:530, 1996.
34. J. Paldus and X. Z. Li. *Advances in Quantum Chemistry*, 110:1–175, 1999.
35. R. J. Bartlett. *Recent Advances in Coupled-Cluster Methods*, volume 3 of *Recent Advances in Computational Chemistry*. World Scientific, Singapore, 1997.
36. R. J. Bartlett. Coupled-cluster theory: An overview of recent developments. In D. R. Yarkony, editor, *Modern Electronic Structure Theory*, pages 1047–1131, Singapore, 1995. World Scientific.
37. M. Head-Gordon, M. Oumi, and D. Maurice. *Mol. Phys.*, 96:593–574, 1999.
38. M. Head-Gordon, R. J. Rico, M. Oumi, and T. J. Lee. *Chem. Phys. Lett.*, 219:21–29, 1994.
39. J. Schirmer. *Phys. Rev. A*, 26:2395–2416, 1981.
40. A. B. Trofimov and J. Schirmer. *J. Phys. B*, 28:2299–2324, 1995.
41. E. S. Nielsen, P. Jørgensen, and J. Oddershede. *J. Chem. Phys.*, 73:6238–6246, 1980.
42. M. J. Packer, E. K. Dalskov, T. Enevoldsen, H. J. A. Jensen, and J. Oddershede. *J. Chem. Phys.*, 105:5886–5900, 1980.
43. O. Christiansen, K. L. Bak, H. Koch, and S. P. A. Sauer. *Chem. Phys. Lett.*, 284:47–55, 1998.
44. A. I. Krylov, C. D. Sherrill, E. F. C. Byrd, and M. Head-Gordon. *J. Chem. Phys.*, 109:10669–10678, 1998.
45. T. B. Pedersen, H. Koch, and C. Hättig. *J. Chem. Phys.*, 110:8318–8327, 1999.
46. K. Raghavachari, G. W. Trucks, J. A. Pople, and M. Head-Gordon. *Chem. Phys. Lett.*, 157:479, 1989.
47. H. Koch, O. Christiansen, P. Jørgensen, A. Sánchez de Merás, and T. Helgaker. *J. Chem. Phys.*, 106:1808, 1997.
48. O. Christiansen, H. Koch, and P. Jørgensen. *J. Chem. Phys.*, 105:1451–1459, 1996.
49. O. Christiansen, H. Koch, and P. Jørgensen. *J. Chem. Phys.*, 103:7429–7441, 1995.
50. C. Hättig and A. Köhn. *J. Chem. Phys.*, 117:6939–6951, 2002.
51. J. L. Whitten. *J. Chem. Phys.*, 58:4496–4501, 1973.
52. B. I. Dunlap, J. W. D. Connolly, and J. R. Sabin. *J. Chem. Phys.*, 71:3396–3402, 1979.
53. O. Vahtras, J. E. Almlöf, and M. W. Feyereisen. *Chem. Phys. Lett.*, 213:514–518, 1993.
54. M. W. Feyereisen, G. Fitzgerald, and A. Komornicki. *Chem. Phys. Lett.*, 208:359–363, 1993.
55. F. Weigend and M. Häser. *Theor. Chem. Acc.*, 97:331, 1997.
56. F. Weigend, M. Häser, H. Patzelt, and R. Ahlrichs. *Chem. Phys. Letters*, 294:143, 1998.
57. A. P. Rendell and T. J. Lee. *J. Chem. Phys.*, 101:400–408, 1994.
58. K. Eichkorn, O. Treutler, H. Öhm, M. Häser, and R. Ahlrichs. *Chem. Phys. Lett.*, 240:283–289, 1995. Erratum ibid. 242 (1995) 652.
59. F. Weigend, A. Köhn, and C. Hättig. *J. Chem. Phys.*, 116:3175, 2001.

60. C. Hättig. *Phys. Chem. Chem. Phys.*, 7:59–66, 2005.
61. TURBOMOLE, Program Package for ab initio Electronic Structure Calculations , `http://www.turbomole.com`.
62. A. Köhn and C. Hättig. *Chem. Phys. Lett.*, 358:350–353, 2002.
63. T. H. Dunning. *J. Chem. Phys.*, 90:1007–1023, 1989.
64. A. Schäfer, H. Horn, and R. Ahlrichs. *J. Chem. Phys.*, 97(4):2571–2577, 1992.
65. A. Schäfer, C. Huber, and R. Ahlrichs. *J. Chem. Phys.*, 100(8):5829–5835, 1994.
66. F. Weigend, F. Furche, and R. Ahlrichs. *J. Chem. Phys.*, 119:12753–12762, 2003.
67. R. A. Kendall, T. H. Dunning, and R. J. Harrison. *J. Chem. Phys.*, 96:6796–6806, 1992.
68. D. E. Woon and T. H. Dunning. *J. Chem. Phys.*, 98:1358–1371, 1993.
69. D. E. Woon and T. H. Dunning. *J. Chem. Phys.*, 100:2975–2988, 1994.
70. A. K. Wilson, D. E. Woon, K. A. Peterson, and T. H. Dunning. *J. Chem. Phys.*, 110:7667–7676, 1999.
71. T. H. Dunning, K. A. Peterson, and A. K. Wilson. *J. Chem. Phys.*, 114:9244–9253, 2001.
72. K. A. Peterson and T. H. Dunning. *J. Chem. Phys.*, 117:10548–10560, 2002.
73. C. Hättig and A. Köhn. *J. Chem. Phys.*, 117:6939–6951, 2002.
74. C. Hättig and F. Weigend. *J. Chem. Phys.*, 113:5154–5161, 2000.
75. C. Hättig. *J. Chem. Phys.*, 118:7751–7761, 2003.
76. C. Hättig, A. Hellweg, and A. Köhn. *Phys. Chem. Chem. Phys.*, 2005. submitted for publication.
77. A. Köhn and C. Hättig. *J. Chem. Phys.*, 119:5021–5036, 2003.
78. P. Pulay, S. Saebø, and K. Wolinski. *Chem. Phys. Lett.*, 344:543, 2001.
79. W. J. Hehre, R. Ditchfield, and J. A. Pople. *J. Chem. Phys.*, 56:2257, 1972.
80. G. E. Scuseria. *Chem. Phys. Lett.*, 176:423, 1991.
81. M. Häser, J. Almlöf, and G. E. Scuseria. *Chem. Phys. Lett.*, 181:497–500, 1991.
82. K. Hedberg, L. Hedberg, D. S. Bethune, C. A. Brown, H. C. Dorn, R. D. Johnson, and M. De Vries. *Science*, 254:410–412, 1991.
83. C. S. Yannoni, P. P. Bernier, D. S. Bethune, G. Meijer, and J. R. Salem. *J. Am. Chem. Soc.*, 113:3190, 1991.
84. J. M. Hawkins, A. Meyer, T. A. Lewis, S. Lorin, and F. J. Hollander. *Science*, 252:312, 1991.
85. J. P. Perdew. *Phys. Rev. B*, 33(12):8822–8824, 1986.
86. J. P. Perdew. *Phys. Rev. B*, 34:7046, 1986.
87. A. D. Becke. *Phys. Rev. A*, 38(6):3098–3100, 1988.
88. F. Furche, 2005. Private communication.
89. B. V. Lebedev, L. Y. Tsvetkova, and K. B. Zhogova. *Thermochimica Acta*, 299:127–131, 1997.
90. A. Köhn and C. Hättig. *J. Am. Chem. Soc.*, 126:7399–7410, 2004.
91. A. Hellweg, C. Hättig, and A. Köhn. *J. Am. Chem. Soc.*, 2005. submitted for publication.
92. W. Rettig, B. Bliss, and K. Dirnberger. *Chem. Phys. Lett.*, 305:8–14, 1999.
93. K. A. Zachariasse. *Chem. Phys. Lett.*, 320:8–13, 2000.
94. K. A. Zachariasse, S. I. Druzhinin, W. Bosch, and R. Machinek. *J. Am. Chem. Soc.*, 126:1705–1715, 2004.

95. S. Techert and K. Zachariasse. *J. Am. Chem. Soc.*, 126:5593–5600, 2004.
96. T. Yoshihara, S. Druzhinin, and K. Zachariasse. *J. Am. Chem. Soc.*, 126:8535–3539, 2004.
97. W. Fuß, K. K. Pushpa, W. Rettig, W. E. Schmid, and S. A. Trushin. *Photochem. Photobiol. Sci.*, 1:255–262, 2002.
98. S. Zilberg and Y. Haas. *J. Phys. Chem. A*, 106:1–11, 2002.
99. W. M. Kwok, C. Ma, P. Matousek, A. W. Parker, D. Phillips, W. T. Toner, M. Towrie, and S. Umapathy. *J. Phys. Chem. A*, 105:984–990, 2001.
100. J. Dreyer and A. Kummrow. *J. Am. Chem. Soc.*, 122:2577–2585, 2000.
101. D. Rappoport and F. Furche. *J. Am. Chem. Soc.*, 126:1277–1284, 2004.
102. A. Köhn. PhD thesis, Universität Karlsruhe, 2003.
103. C. Bulliard, M. Allan, G. Wirtz, E. Haselbach, K. A. Zachariasse, N. Detzer, and S. Grimme. *J. Phys. Chem. A*, 103:7766–7772, 1999.
104. U. Lommantzsch, A. Gerlach, C. Lahmann, and B. Brutschy. *J. Phys. Chem. A*, 102:6421–6435, 1998.
105. W. Schuddeboom, S. A. Jonker, J. M. Warman, U. Leinhos, W. Kühnle, and K. A. Zachariasse. *J. Phys. Chem.*, 96:10809–10819, 1992.
106. A. B. J. Parusel, G. Köhler, and S. Grimme. *J. Phys. Chem. A*, 102:6297–6306, 1998.
107. S. A. Trushin, T. Yatsuhashi, W. Fuß, and W. E. Schmid. *Chem. Phys. Lett.*, 376:282–291, 2003.
108. T. Yatsuhashi, S. A. Trushin, W. Fuß, , W. Rettig, W. E. Schmid, and S. Zilberg. *Chem. Phys.*, 296:1, 2004.
109. W. Fuß, W. Rettig, W. E. Schmid, S. A. Trushin, and T. Yatsuhashi. *Farad. Disc.*, 127:23, 2004.
110. W. Fuß, 2005. private communication.